UNIVERSITAT POLITÈCNICA DE CATALUNYA
BARCELONATECH
Escola d'Enginyeria de Barcelona Est

FINAL MASTER'S THESIS

Master's degree in Chemical Engineering
Smart Chemical Factories

Risk Analysis of Triethylaluminium Storage

Author: Tanaz Moghadamfar

Director: Elsa Pastor

Codirector: Eulalia Planas Cuchi

Call: June 2022

Abstract

In this century, the global consumption of hazardous materials has risen. This is because, in recent years, industry attitudes regarding hazardous compounds, which are key components of many essential commercial goods, have changed significantly. These materials demand extra caution since they can have serious health and environmental consequences. The main goal of this thesis is to identify and analyze the hazards of storing pyrophoric substances that exposure to the environment or other materials at ambient temperatures can cause these materials to ignite. These analyses are used to develop the storage and handling hazards.

Among all the pyrophoric chemicals regularly employed in industry, Triethyl aluminum (TEA) has piqued this thesis's attention in terms of its wide range of uses as an efficient catalytic component, an additive with fuel for micro-encapsulation, in aircraft design, and in the military area. TEA is basically prepared from aluminum, hydrogen, and ethylene in a one or two-step process. TEA is a colorless liquid that self-ignites and reacts violently with air and water. As a result, high heat and combustible gases such as hydrogen will be released, the concentration of which increases as the system temperature rises.

The processing industries and related operations for TEA as a hazardous commodity are exposed to the risk of various serious accidents, such as pool fires caused by fuel spills which is one of the most prevalent unintentional incidents in an industrial setting. The damages caused by a TEA fire are mainly connected to the heat radiated in the surrounding area. So, in order to analyze and predict the expected hazards of neat TEA and its solution storage, the heat received by a given target was computed using various classical equations, the most frequent of which are compiled in this thesis. At the same time, experimental data for neat TEA and its solutions has also been collected to be compared.

The empirical fire modeling is a generalized practice due to its ability to quickly generate accurate estimations of general fire conditions. However, performing these experiments is sometimes too risky for hazardous substances like TEA. So, in order to analyze the TEA solutions storage risk, a less hazardous substitute material should be introduced that is expected to have a similar pool fire behavior in terms of the flame geometry. Accordingly, the Fire Dynamic Simulation (FDS) has been performed for different hydrocarbon chemicals to find the best substitution for TEA solutions for further experiments. N-hexane, n-octane, and benzene have been chosen based on the similarity and close heat of combustion, vaporization, and mass burning rate compared to TEA solution. Finally, in line with the results obtained, the performance of a fire protection system in a TEA storage facility has been analyzed for its practical implementation.

Resumen

En este siglo, el consumo global de materiales peligrosos ha aumentado. Esto se debe a que, en los últimos años, las actitudes de la industria con respecto a los compuestos peligrosos, que son componentes clave de muchos bienes comerciales esenciales, han cambiado significativamente. Estos materiales exigen una precaución especial ya que pueden tener graves consecuencias para la salud y el medio ambiente. El objetivo principal de esta tesis es identificar y analizar los peligros del almacenamiento de sustancias pirofóricas, a las que la exposición al aire y al agua puede provocar la ignición.

Entre todos los productos químicos pirofóricos empleados regularmente en la industria, el trietilaluminio (TEA) ha llamado la atención de esta tesis en términos de su amplia gama de usos como un componente catalítico eficiente, un aditivo con combustible para microencapsulación, en el diseño de aeronaves y en aplicaciones militares. El TEA se obtiene básicamente a partir de aluminio, hidrógeno y etileno en un proceso de uno o dos pasos. El TEA es un líquido de incoloro que se auto inflama y reacciona violentamente con aire y agua. Como resultado, se liberarán gases combustibles a alta temperatura como hidrógeno, cuya concentración aumenta a medida que aumenta la temperatura del sistema.

Las industrias de procesamiento y las operaciones relacionadas con el TEA están expuestas al riesgo de varios accidentes graves, como incendios de balsa causados por derrames de combustible, que es uno de los incidentes no intencionales más frecuentes en un entorno industrial. Los daños causados por un incendio de TEA están relacionados principalmente con el calor irradiado en el área circundante. Entonces, para analizar y predecir los peligros esperados del TEA puro y su almacenamiento en solución, Se ha marcado como objetivo de esta tesis el cálculo de calor recibido por un objetivo determinado.

El modelado experimental de incendios es una técnica habitual utilizada para generar rápidamente estimaciones de las condiciones generadas en un incendio. Sin embargo, realizar estos experimentos a veces es demasiado arriesgado para sustancias peligrosas e inflamables como el TEA. Por lo tanto, para analizar experimentalmente el riesgo de almacenamiento de soluciones de TEA, se debe introducir un material sustituto menos peligroso que se espera que tenga un comportamiento similar al fuego en términos de geometría de la llama. Ha sido pues también objeto de esta tesis realizar la simulación dinámica de incendios mediante la herramienta computacional FDS para diferentes productos químicos de hidrocarburos para encontrar la mejor sustitución de soluciones de TEA. El N-hexano, el n-octano y el benceno se han elegido en función de la similitud por lo que hace referencia al calor de combustión, la vaporización y la velocidad de combustión con la solución de TEA.

Finalmente, en base a los resultados obtenidos, se ha analizado la adecuación de un sistema industrial de protección de incendios para su implementación en plantas de almacenaje de soluciones de TEA.

Acknowledgements

First and foremost, I would like to express my deepest gratitude to my project director, Elsa Pastor, and project co-director, Eulalia Planas Cuchi, for their guidance and support throughout the entire project at the research group the CERTEC (Centre d'Estudis del Risc Tecnològic).

I would like to extend my gratitude to all the members from CERTEC, for their commitment and welcoming attitude towards me when I first join the group. Particularly, I would like to express my appreciation to Alba Agueda, for all her supports and knowledge provided me with respect.

Furthermore, much love and thanks to my parents who are the source of my happiness: it is the unfailing support of my family that has enabled me to complete this Masters project. Their support during the entire studies has given me strength in the most challenging moments. Thank you all.

Glossary

NFPA	National Fire Protection Association
GHS	Globally harmonized system
CFD	Computational Fluid Dynamics
SDS	Safety Data Sheet
FDS	Fire Dynamic Simulation
HRRPUL	Heat release rate per unit length
Acc. HRRPUL	Accumulated heat release rate per unit length
Et	Ethyl
PET	Polyethylene terephthalate
PVC	Polyvinyl chloride
PLA	Polylactic acid
PHB	Poly-3-hydroxybutyrate
T_m	Melting temperature
$\dot{m}"$	Fuel mass burning rate
A	Spill fire area
y'	Fuel burning regression rate
ρ	Density of the fuel
$\dot{m}"_\infty$	The specific mass burning rate at ''infinite'' diameter
K	The absorption-extinction coefficient of the flame
β	The correction coefficient for the beam length
D	The pool diameter
ΔH_v^*	Modified heat of vaporization at the boiling point of liquid
ΔHc	Heat of combustion
ΔHv	Heat of vaporization

C_p	Specific heat capacity of the liquid
T_b	Boiling temperature
T_a	Ambient temperature
L_f	The 50-percentile intermittent flame height
Q_r	The heat release rate
H	Average flame length
ρ_a	Ambient air density
g	Gravitational acceleration
SEP_{max}	Maximum Surface Emissive Power from a flame without soot production
F_s	Fraction of the combustion energy radiated from the flame surface
L	Average flame height
E	Equivalent emissive power
E_{max}	Equivalent blackbody emissive power
s	Extinction coefficient
E_s	Emissive power of smoke
σ	The Stefan-Boltzmann constant
ε	The emissivity which depends on the substance present in the flame
T_{fl}	The radiation temperature of the flame
T_a	The ambient temperature
η_{rad}	The radiative fraction or radiant heat fraction
A	The area of the solid flame from which radiation is released
τ	The atmospheric transmissivity
d	The distance between the surface of the flame and the target
p_w	The partial pressure of water in the atmosphere
H_R	The relative humidity of the atmosphere

p_{wa}	The saturated water vapor pressure at the atmospheric temperature
L	Distance between the center of the cylinder to the target
H	Height of the cylinder
D	Cylinder diameter
F_H	Horizontal view factor
F_V	Vertical view factor
F_{max}	Maximum view factor
Q''	Heat flux of pool fire
E	Average emissive power at flame surface
I	The thermal radiation intensity
l_p	The distance between the point source and the target
φ	The angel between the plane perpendicular to the receiving surface and the line joining the source point and the target
E_{lum}	Luminous zone's emissive power
E_{soot}	Non-luminous zone's emissive power

Index

Preface

Project motivation

In process plants, accidents involving fires are among the most common major accidents. In a plant handling hazardous chemical, the major hazard arises from the storage, handling, and use of these chemicals. When these dangerous chemicals are released into the atmosphere, they may cause damage due to subsequent fires. Irrespective of the source, most agree that pool fires are one of the most common accidents in industry (Casal, 2012). Analyzing the risk associated to hazardous substances pool fires have always been interesting to fire and safety engineers. Identification of the characteristics and behavior of these substances in case of ignition, as well as their possible consequences, is the first step in mitigating the risks.

Risk analysis is the process of identifying and analyzing potential issues that could adversely affect key business initiatives or projects. An organization can improve its security in a number of ways by conducting a risk analysis. The results of a risk analysis can be used in a variety of ways, depending on the type and extent of the study (Aven, 2016):

- Assess, rate, and compare the overall impact of risks on the organization
- Enhance safety policies and procedures and implement this information in security policies and procedures in a cost-effective manner
- Put security controls in place to minimize and extinguish the most significant risks
- Raising employee awareness of security measures and risks through the use of best practices during the risk analysis process
- Know the potential financial impact of security risks
- Land-use planning and emergency planning and management

Project objectives

This thesis aims to analyze the risks associated with storing triethyl aluminum (TEA) and recommend a substitution substance for future fire protection system tests.

The goal of this research features three independent but interrelated parts: Firstly, it was aimed to analyze the existed analytical modeling in literature to predict the radiation heat and flame geometry of a large TEA pool fire caused by a storage tank loss of containment. To this end, theoretical models have to be analyzed for TEA and its solutions to compare various correlations' accuracy and to find the best approach for them. The second objective deals with the need to find a less risky hydrocarbon

chemical with a close fire behavior to TEA solution in terms of flame geometry that can be handled easier for fire experimentation. Computational fire dynamic simulations are the selected approach to investigate the best possible proxy for TEA from n-hexane, n-octane, and benzene. Finally, the investigation of the performance of a fire protection system will be done for TEA solution pool fires to be implemented in industrial storage facilities.

1. Introduction to pyrophoricity

Pyrophoricity is the characteristic of those materials that react violently with oxygen at room temperature in air. The energy that can be released in this oxidation is so high that the materials ignite themselves. Pyrophoric materials often react violently also with moisture and water, usually emitting flammable gases (i.e., hydrogen) at a high rate. But on the other hand, these chemicals can be useful and essential to catalyze certain reactions, be incorporated into final products, or also can be used in organic synthesis in many industrial applications (UNL, 2009).

The materials which generally have the mentioned properties can be named as pyrophoric substances and since in Greek pyr means fire and phorein means to carry, it refers to a substance that carries fire. Pyrophoricity is a dangerous and undesirable phenomenon that hampers the production and use of materials. Clearly the primary risk associated with these pyrophoric substances is ignition, fires and explosion which can occur in the event of an unexpected loss of containment (e.g., during shutdowns when tanks or vessels are emptied or equipment and piping are opened for inspections and maintenance (Heyn, 2015).

Pyrophoric properties depend on the chemical nature of materials, their mass, particle size, particle shape, surface morphology, and the presence of protective coating (Alymov et al., 2020). Pyrophoric substances may be solids (powders), liquids, solutions in inert solvents or gases, but most pyrophoric materials are solid metals. Pyrophoricity is a special case of a hypergolic reaction because the oxidizing agent is restricted to atmospheric oxygen. Whereas pyrophoricity is concerned only with the spontaneous combustion of a material when exposed to air (atmospheric oxygen), a hypergolic reaction describes the ability of a material to spontaneously ignite or explode upon contact with any oxidizing agent (Leong & Edwards, 2020).

1.1. Pyrophoric substances

Pyrophoric substance groups which are listed in **Table 1**, based on their diversity will be classified to three main groups of gas, liquid and solid.

Table 1. *Pyrophoric substance groups and typical examples* (Heyn, 2015).

Pyrophoric substance group	Typical example
Metal alkyls and aryls	Triethylaluminium, (n-, sec-, tert-) butyllithium, diethylzinc, dimethyl cadmium
Grignard Reagents	R Mg X (R=alkyl, X=halogen), methyl magnesium bromide
Metal carbonyls	Iron pentacarbonyl, nickel tetracarbonyl
Metal hydrides	Sodium hydride, lithium aluminum hydride
Non-metal alkyls	R3B, R3P, R3As, tributyl phosphine
Non-metal hydrides	Diethyl arsine, diethyl phosphine
Metal powders (finely divided)	Cobalt, iron, zinc, zirconium, hafnium
Alkali and partially alkaline earth metals	Lithium, sodium, potassium, rubidium, cesium; calcium, strontium, barium
White phosphorus	
Pyrophoric gases	(Mono-, di-) silane, di-chlorosilane, diborane, phosphine, arsine

1.1.1 Pyrophoric gases

National Fire Protection Association (NFPA) standards use the term "pyrophoric gases". Instead, in Globally Harmonized System (GHS) categorization, gases that ignite on exposure to air will be listed as "Flammable gases". Diborane, arsine, phosphine, and silane can be counted as the most commonly used pyrophoric gases in the industry, which may ignite on exposure to air depending on humidity and temperature. Generally, all are toxic by inhalation, but some, like phosphine, are highly toxic. Silane will ignite when exposed to air under most environmental conditions, and diborane will ignite spontaneously in moist air (UNL, 2009).

All of the gases that are mentioned in the **Table 1** as pyrophoric gases and many other compounds that contain these gases in their molecular structure can ignite immediately upon exposure to air and are all nonmetallic hydrides.

Arsine (AsH_3), also known as an arsenic hydride, is a colorless, highly toxic gas with a distinctive garlic-like odor. It is heavier than air and is a blood and nerve poison. Arsine will generally not ignite in the air unless at elevated temperatures, but it can be detonated by a suitably powerful initiation (heat source, shock wave, electrostatic discharge). Arsine may also exist in other compounds. The ignition temperature of many of these arsine-containing compounds is lower than that of arsine, causing them to ignite in the air even at low temperatures (below 0 °C). All arsine compounds should be considered pyrophoric until they are adequately characterized (Sam Mannan; Harry H west, 1999).

Silane (SiH_4), also known as silicon tetrahydride, is a colorless gas with a putrid odor. It and its compounds (e.g., di-silane) can ignite in air and react violently with chlorine. The presence of other hydrides as impurities causes the ignition to occur in the air. However, 99.95% pure silane generally ignites in the air only when emerging at very high gas velocities, whereas mixtures of up to 10% silane may not ignite. Hydrogen liberated from its reaction with air (atmospheric oxygen) often ignites explosively. Silanes react violently with chlorine and bromine. All silanes should be considered pyrophoric until they are adequately characterized (Sam Mannan; Harry H west, 1999).

1.1.1. Pyrophoric liquids

Pyrophoric liquids are present in two forms, pure liquids and solutions. Examples of pure liquids include diethylzinc, triethylaluminium, trimethylaluminum, triethyl borane, and tributyl phosphine. Mixtures typically contain metal alkyl substances such as ethyl lithium, methyllithium, n-butyllithium, sec-butyllithium, and t-butyllithium dissolved in a solvent such as hexane, pentane, diethyl ether or tetrahydrofuran. Pyrophoric liquids are typically packaged in glass bottles under an inert atmosphere, such as dry nitrogen or argon, and sealed to prevent air intrusion (Alnajjar et al., 2011).

Alkyl-aluminum is one of the most common pyrophoric liquids. Typically, metal alkyl compounds are used within the chemical industry as catalysts in many organic chemical reactions. They are usually pyrophoric, upon contact with air they lead to self-ignition with the formation of harmful gases which are often irritating to the respiratory system. Metal alkyl compounds tend to react extremely vigorously with water generating intense heat and releasing flammable gases. It is important to bear in mind that hazardous reactions can occur with organic acids, esters, alcohols, aldehydes, ketones, amines, amides, ethers, hydrogen halides, etc.

Hydrazine is a colorless oily liquid resembling water in appearance and possesses a weak, ammonia-like odor. Its chemical formula is N_2H_4. Commercially it is available as a hydrous (without water)

liquid and in aqueous solutions. Hydrazine is most well-known for its use as a rocket fuel, but is also used in manufacturing agricultural chemicals, explosives, and plastics. It fumes in air and reacts with all oxidizing agents.

Hydrazine is hypergolic, meaning that it reacts explosively upon contact with many oxidizing agents. The flash point of hydrazine is 38 °C. Its autoignition temperature is 270 °C on a glass surface but may be as low as 23°C when in contact with a strong oxidizing agent. Hydrazine forms flammable mixtures with air from 4% to 100% by volume and decomposes when heated. Hydrazine ignites in the air at room temperature when exposed to metal oxide surfaces and in a wide variety of porous materials.

1.1.2. Pyrophoric solids

Pyrophoric solids form the most percentage of pyrophoric substances, which examples are alkali metals (such as potassium, sodium), finely divided metal powders (aluminum, cobalt, iron, magnesium, titanium, zirconium, zinc), metal hydrides (sodium hydride, lithium aluminum hydride), alloys of reactive metals (sodium–potassium alloy) and white phosphorus.

Nearly all solid metals will burn in air under certain conditions. Some are oxidized rapidly in the presence of air or moisture, generating sufficient heat to reach their ignition temperatures. Others oxidize so slowly that heat generated during oxidation is dissipated before the metal becomes hot enough to ignite. Hot or burning metals may react violently upon contact with other materials, such as oxidizing agents and extinguishing agents used on fires involving ordinary combustibles or flammable liquids(Alnajjar et al., 2011).
Properties of burning metal fires cover a wide range. Burning titanium produces little smoke, while burning lithium smoke is dense and profuse. Some water-moistened metal powders, such as zirconium, burn with near explosive violence, while the same powder wet with oil burns quietly. Sodium melts and flows while burning; calcium does not. Some metals (e.g., uranium) acquire an increased tendency to burn after prolonged exposure to moist air, while prolonged exposure to dry air makes it more difficult to ignite.

One of the most common pyrophoric materials in industry is pyrophoric iron sulfide, which is created when iron oxide (rust) is converted into iron sulfide. This chemical reaction only takes place in low oxygen conditions. When the pyrophoric iron sulfide particles are exposed to air, they are oxidized back to iron oxide, generating a considerable amount of heat. So much heat is produced that the particles can burn, igniting nearby flammable hydrocarbon gases (Gao et al., 2017a).

Iron sulfide deposits on the tank walls were exposed to the gases inside the tanks when the liquid levels in the tanks dropped. The oxygen interacted with the vapors and gases in the tanks to generate an explosive environment, and then oxygen reacted with the pyrophoric iron sulfide to provide a source

of ignition. The explosive environment was then ignited by the pyrophoric iron sulfide, resulting in catastrophic damage (Gao et al., 2017b).

Tanks that have been sitting empty for a long time can still be dangerous. When exposed to oxygen, pyrophoric iron sulfide can persist on tank walls for long periods of time before igniting. Therefore, when working with pyrophoric iron sulfide, various precautions must be taken to avoid an explosion (Kong et al., 2016).

1.2. Handling of pyrophoric substances

The GHS stands for Globally Harmonized System of classification and labeling of chemicals. A system for harmonizing classification criteria and chemical hazard communication elements across the globe. The GHS is not a regulation; rather, it is a framework or guide for classifying and labeling hazardous chemicals. A GHS classification is intended to provide harmonized information to users of chemicals to enhance protection of human health and the environment (GHS, 2010). GHS consists of three major hazard groups: Physical, health and environmental hazard. These hazard groups are further subdivided into classes and categories, which are outlined in **Table 2** and **Table 3**. The GHS classes can also be rated and categorized from 1 to 4, where category 1 corresponds to the most severe and 4 to the least severe (GHS, 2009).

Table 2. *GHS hazmat classification for physical hazard* (GHS, 2009).

Physical hazard			
1. Explosives	6. Flammable liquids	11. Self-heating substances and mixtures	16. Corrosive to metals
2. Flammable gases	7. Flammable solids	12. Substances and mixtures which, in contact with water, emit flammable gases.	17. Desensitized explosives
3. Aerosols	8. Self-reactive substances and mixtures	13. Oxidizing liquids	
4. Oxidizing gases	9. Pyrophoric liquids	14. Oxidizing solids	
5. Gases under pressure	10. Pyrophoric solids	15. Organic peroxides	

Table 3. *GHS hazmat classification for health and environmental hazard* (GHS, 2009).

Health hazard		Environmental hazard
1. Acute toxicity	6. Carcinogenicity	11. Hazardous to the aquatic environment (acute and chronic).
2. Skin corrosion/irritation	7. Reproductive toxicity	12. Hazardous to the ozone layer
3. Serious eye damage/eye irritation	8. Specific target organ toxicity - single exposure	
4. Respiratory or skin sensitization	9. Specific target organ toxicity - repeated exposure	
5. Germ cell mutagenicity	10. Aspiration hazard	

In physical hazard classification numbers from 6 to 12 can be correlated to the burning behavior of pyrophoric materials. In terms of health hazards, there are corrosivity, teratogenicity, and organic peroxide formation, as well as damage to the liver, kidneys, and central nervous system. Regarding environmental hazards, no specific information has been found for this substance. In addition, pyrophoric substances will include in the Safety Data Sheet (SDS) one of the hazard statements indicated below (UNL, 2009):

- H250 Catches fire spontaneously if exposed to air
- H260 In contact with water releases flammable gases which may ignite spontaneously
- H261 In contact with water releases flammable gas

Pyrophoric substances should be kept in small quantities and stored in an inert gas or kerosene atmosphere, as applicable. Avoid areas with heat or flames, as well as oxidizers and water sources. The accurate chemical identity and hazard warning must be clearly labeled on containers transporting pyrophoric compounds. It's critical not to let pyrophoric compounds that have been stored in solvent dry out. They should also be examined on a regular basis to verify that there is still a visible amount of solvent in the bottle. However, different procedures and strategies should be used depending on the type of substance and its qualities (Alnajjar et al., 2011).

When dealing with fires involving flammable gases, the best course of action is to turn off the gas supply before attempting to put out the fire. Extinguishing the fire while allowing the gas to flow is

exceedingly risky; an explosive cloud of gas and air could form, causing significantly more damage than the original fire if ignited. To provide fast access to valves to cut off the flow of gas, extinguishing the flame with carbon dioxide or a dry chemical may be beneficial, but this must be done carefully. In many cases, it will be preferable to allow continued burning, while protecting exposures with water spray, until the flow of gas can be stopped. Since many pyrophoric gases react violently with halogens, halons should not be used as extinguishing agents (Mellon, 2019).

Fires involving pyrophoric liquids like hydrazine can produce irritants and poisonous gases such as nitrogen oxides. Protective clothes and positive pressure respirators should be worn when approaching a fire. To avoid harmful fumes and poisonous decomposition products, approach these fires from the upwind side. Flooding water should be applied in the form of a fog or spray. To keep fire-exposed containers cool, sprinkle them with water. Fires should be battled from a safe distance or from a protected area. To prevent re-ignition, large amounts of water may be required (M. Sam; Harry. W, 1999).

Since pyrophoric solids are more stable in air than pyrophoric liquids and gases, some manufacturers sell formulas that do not require an inert atmosphere until right before use. Sodium hydride and lithium aluminum hydride, for example, are marketed as powders blended with mineral oil (dispersions). Metals like potassium and sodium are sometimes sold in huge chunks submerged in mineral oil. To use these materials, simply measure out the amount needed, place it in an inert environment, then wash it with a solvent such as hexane several times to remove the mineral oil (Alnajjar et al., 2011).

The toxicity of certain solid metals has implications in firefighting as well. If metals (particularly heavy metals) enter the bloodstream or their smoke fumes are inhaled, they can be poisonous or lethal. Metal fires should never be approached without the appropriate safety gear (clothing and respirators). Ionizing radiation is emitted by a few metals, such as thorium, uranium, and plutonium, which can hamper firefighting and cause radioactive pollution. Because of the risk of extensive radioactive contamination during a fire, radioactive materials should not be processed or stored with other pyrophoric compounds. Where such combinations are critical to operations, engineering controls and emergency procedures should be in place to avoid fires or quickly extinguish fires if the controls fail. Because extinguishing fires in flammable metals necessitates procedures not frequently used in traditional firefighting operations, people in charge of putting out combustible metal fires must be carefully taught prior to a real incident (Alnajjar, 2009).

In general, it is crucial to remember that if any pyrophoric compound is spilled, powdered lime should be used to totally smother and cover the spill. When working with pyrophoric materials, keep a container of powdered lime within arm's reach (Technical Bulletin AL-164, 1995).

Hazardous garbage should be disposed of any materials that contain or are contaminated with pyrophoric substances. In this instance, adequate and full hazardous waste container labeling is essential, and the container containing residual substance should never be opened to the atmosphere. If the pyrophoric chemical was previously stored in a solvent and has dried up, it should be rehydrated with the appropriate solvent before being picked up. The best solvent is the same one that was used to dissolve the initial reagent (Technical Bulletin AL-164, 1995).

2. Introduction to Triethylaluminium (TEA)

Triethylaluminium, with the formula of $Al_2(C_2H_5)_6$ (abbreviated as Al_2Et_6 or TEA), is one of the simplest examples of aluminum alkyls that referred to a family of organo-aluminum (Irving Sax, 1988). Triethylaluminium can be formed via several routes. The multistep process uses aluminum metal, hydrogen gas, and ethylene and follows the reaction:

$$2\,\mathrm{Al} + 3\,\mathrm{H_2} + 6\,\mathrm{C_2H_4} \rightarrow \mathrm{Al_2}Et_{\,6} \qquad \textit{Equation 1}$$

It can also be generated from ethyl aluminum sesquichloride ($Al_2Cl_3Et_3$), which arises by treating aluminum powder with chloroethane. Reduction of ethyl aluminum sesquichloride with an alkali metal such as sodium gives triethylaluminium:

$$6\,\mathrm{Al_2Cl_3Et_{\,3}} + 18\,\mathrm{Na} \rightarrow 3\,\mathrm{Al_2Et_{\,6}} + 6\,\mathrm{Al} + 18\,\mathrm{NaCl} \qquad \textit{Equation 2}$$

TEA is a colorless pyrophoric liquid that leads to self-ignition and tends to react extremely violently with water, generating intense heat and releasing flammable gases like hydrogen, which content rises as the system temperature increases. Explosive reactions can occur when reacting with alcohols, carbon tetrachloride, and n-dimethyl in the presence of heat (Irving Sax, 1988).

Triethylaluminium (TEA) is one of the few substances sufficiently pyrophoric to ignite in contact with cryogenic liquid oxygen. Its ease of ignition makes it particularly desirable as a rocket engine ignitor, and its flares' high energy density and reactivity make them useful in military aircraft. In addition, TEA is employed in the Ziegler Natta polymerization of olefins, as well as in the manufacture of various organometallic compounds and organic intermediates models (Gonçalves et al., 2018a).

Furthermore, it is essential to emphasize that, above 120 ºC, TEA decomposes slowly, yielding hydrogen, ethylene, and elemental aluminum as thermal decomposition products. Aluminum oxide is produced during burning, and the smoke may contain different hydrocarbons that might induce severe health hazards. If TEA and its solutions are completely burned, aluminum oxide, carbon dioxide, and water will be created (AkzoNobel TEAL, 2010).

2.1. TEA reactions

Aluminum alkyls are usually used as catalysts for the polymerization of ethylene and propylene. For example, in Ziegler Natta polymerization, a tetrachloro titanium and hydrocarbon solution containing triethylaluminium (TEA) polymerizes ethylene under atmospheric pressure (Cotton & Wilkinson, 1972; Streitwieser & Heathcock, 1989). TEA has also been explored for use in jet engine afterburner sustainers and ramjet igniter systems that is a type of jet engine in which the air drawn in for combustion is compressed (Anderson, 1963; Heck & Johnson, 1962).

Compounds containing alkyl groups of C_4 and below ignite immediately on exposure to air unless they are diluted with a hydrocarbon solvent to concentrations of 10-20% (Mirviss, 1961). These solutions may ignite on prolonged exposure to air because of exothermic autoxidation, which becomes rapid if the solutions are spilled. Alkyl aluminum derivatives up to C_4 react explosively with methanol or ethanol, and TEA with 2-propanol. Mixing aluminum alkyls with chlorinated hydrocarbons is a hazardous procedure because the mixture could undergo uncontrolled decomposition (Mirviss, 1961). A series of experiments on mixtures of several different alkyl aluminum with chlorocarbons individually have been conducted (Urben, 2007). It has been determined that chloroform and carbon tetrachloride may react violently with alkyl aluminum derivatives. Interaction of alkyl aluminum derivatives with chain lengths up to C_9 and liquid water is also explosive. Even though it is understood that aluminum alkyls must be treated carefully, some accidents have occurred because the procedures for handling these are difficult (Mirviss, 1961; Urben, 2007).

TEA reactions are too slow under closed conditions, and it is difficult to estimate the explosive reactions using thermal analysis. The results of different experiments in closed conditions also show that thermal disintegration of TEA appears to be less hazardous (Sato et al., 2011a). The thermal breakdown of aluminum alkyls can result in metallic aluminum, olefin, and hydrogen. Regardless, this reaction takes place at low pressure or with eliminating the gaseous products of decomposition. The primary reaction would generate trimethylaluminum and propylene as intermediate products if the thermal breakdown happened with confined products. The trimethylaluminum would then be decomposed further, and the propylene would be polymerized. Experiments and simulations showed that a closed system containing TEA and water degraded into lower-molecular-weight molecules than the well-known TEA hydrolysis products (Sato et al., 2011a).

In addition, the presence of TEA and aluminum hydroxide in a reaction can cause a significant increase in temperature and pressure. Because aluminum hydroxide contains water as alumina hydrates, it's likely that at high temperatures, aluminum hydroxide became a source of water and contributed to the TEA-water mixing reaction (Sato et al., 2011b).

2.2. Combustion process of TEA

A test was designed for the combustion of pure triethylaluminium in water and air to study the characteristics of triethylaluminium detonation (Liu et al., 2013). Sensitizers such as water and air must be introduced to the combustion test for dispersion and explosion of triethylaluminium to improve the efficiency of detonation. The addition of a sensitizer also ensures that before reacting with oxygen, triethylaluminium combines with the sensitizer and results in inflammable gas. The selection of sensitizers is thus a crucial problem in researching triethylaluminium detonation properties (Liu et al., 2013).

In the design of device of simulation, the test vessel was a wide-mouthed jar, which was broken by the electrical detonator's energy. When triethylaluminium was released, it reacted with ambient water and caused a powerful chemical reaction that resulted in an explosion. The test vessel structure is shown in **Figure 1**.

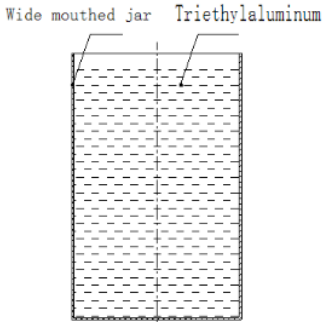

***Figure 1**. Structure of TEA in jar for water sensitization test* (Liu et al., 2013).

The test conditions are summarized in **Table 4**: Each 1200 ml jars were filled with approximately 900 grams of pure triethylaluminium, and a rubber stopper was used to secure and lock the vessel. The jars were then placed in metal basins with 13 liters of water or left dry. Both jars were detonated with electrical detonators and the high-speed photography recorded test phenomenon (Liu et al., 2013).

***Table 4**. Condition and phenomena of water sensitization test* (Liu et al., 2013).

Test number	TEA (Volume L^{-1})	H_2O (Volume L^{-1})	Test phenomena
1	1.15	13	More distinct depression of basin; and significant deformation.
2	1.1	13	
3	1.02	0	No deformation of basin and no depression at the bottom of basin.

High-speed photography revealed that triethylaluminium was burning and dispersing in the air at a maximum dispersion speed of 27($m \cdot s^{-1}$), and triethylaluminium disperses instantly when burning in air. When triethylaluminium was mixed with water, the dispersion speed reached 60 ($m \cdot s^{-1}$), and the chemical reaction began quickly after both were mixed, resulting in a large amount of intermediate product, which presented black cloud clusters wrapping triethyl aluminum (Liu et al., 2013).

As shown in **Figure 2** and **Figure 3**, the range of flame diameter in water was more expanded than in air, horizontally and vertically. After the test ended, the apparent deformation of the aluminum basin could be seen, which indicated overpressure occurred in the reaction process between triethylaluminium and water.

Figure 2**.Reaction of pure TEA mixed with **water (Liu et al., 2013)

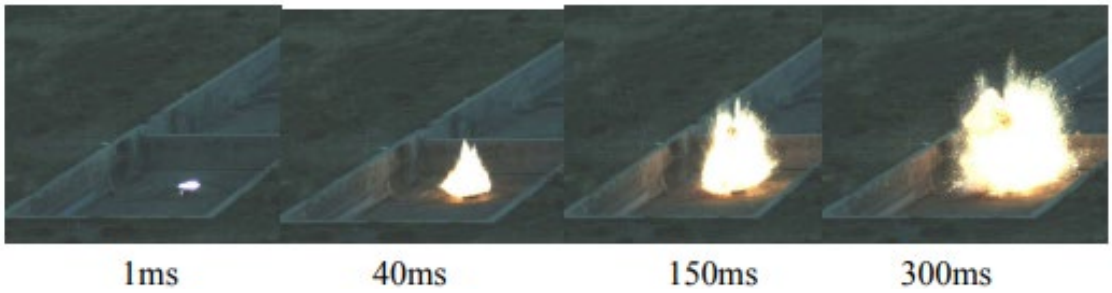

Figure 3**. Reaction of pure TEA mixed with **air (Liu et al., 2013).

In addition, the combustion test of triethylaluminium was performed in different volume of water and the test result shows that appropriately increasing quantity and volume of water facilitates detonation (Liu et al., 2013).

The test conditions are defined as: 2500 ml jars were filled with 1700 grams of triethylaluminium, and they were placed in 50L and 30L vessels of water separately. Two vessels are 600mm and 320mm in diameter respectively and an igniter is located in the center of the vessel. Basically, the height of the water was equivalent to the level of triethylaluminium liquid.

Figure 4 and **Figure 5** are high-speed photographic pictures after explosion in 50L and 30L vessels respectively, and they present different reaction phenomena. It is seen from the high-speed motion

pictures that, with increases in the quantity and volume of water, dispersion decreases vertically while the burning duration and shape of cloud increases. Furthermore, since the test was conducted in open space, the disperse distance, duration of reaction, and disperse speed of the cloud have been increased (Liu et al., 2013).

Due to **Figure 5**, in the test design with 30L vessel, most water has been released out before mixing with triethylaluminium, so proportion of water used to provide combustion was not enough in a large scale. As a result, increasing the amount of water in the vessel and the diameter of the vessel will make detonation easier (Liu et al., 2013).

Figure 4*. Explosive behavior of triethylaluminium in 50L vessel* (Liu et al., 2013).

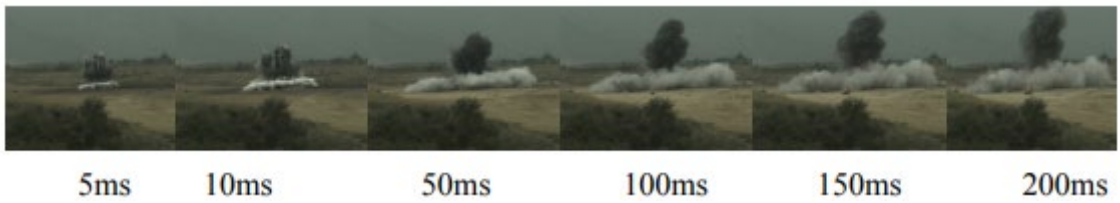

Figure 5 *. Explosive behavior of triethylaluminium in 30L vessel* (Liu et al., 2013)

Due to the high reactivity and the safety precautions that must be taken, the combustion of these materials is usually difficult to be studied experimentally. Therefore, kinetic modeling is essential for deciphering complex reaction pathways (Gonçalves et al., 2018b).

2.3. TEA in industry

Since Ziegler discovered that triethylaluminium was an efficient catalytic component polymerized by olefin, triethylaluminium has piqued the interest of chemists throughout the world in both theory and practice, and the practical issue of large-scale industrial production has been resolved. In 1954, they created triethylaluminium by combining aluminum, hydrogen, and ethylene. With Naty's successful stereo-specific polymerization, the Ziegler-Natta catalyst was born, and the use of triethylaluminium became increasingly popular. From the 1950s through the 1970s, research on triethylaluminium was brisk, and it was mostly mature until the 1970s (Liu et al., 2013).

In addition, in the military field, TEA has been always an interest. It can be employed in order to create a high-temperature flame and burn the target in a variety of ways for example as a fuel in flamethrower, aerial bomb, rocket bombs, rifle grenades and hand grenades (Liu et al., 2013).

Another area in which TEA was employed was in the design of aircrafts. Traveling at the high velocity in the environment poses a number of issues, one of which may be the high stagnation temperatures that are encountered at these high speeds. The capacity to build combustion systems that allow complete combustion in a supersonic flow of combustion is critical to the development of hypervelocity, air breathing vehicles. To put it another way, supersonic combustion necessitates a short ignition latency and rapid reaction speeds which can be provided by addition of TEA to fuel (Ryan et al., 1992).

Pyrophoric organometallic compounds were investigated as an ignition source and flame stabilizing mechanism within the combustor, allowing supersonic combustion systems to employ hydrocarbon fuels. NASA chose TEA as the additive with fuel for microencapsulation because of its strong reactivity and energy density, as well as the fact that it is widely available (Ryan et al., 1992).

2.4. Handling of TEA

Exposure to TEA may cause severe eye and skin irritation and burns, or breathing them can irritate the nose and throat, causing coughing and wheezing. Physical and health hazard identifications are shown in **Table 5**. Corresponded hazards are selected from **Table 2** and **Table 3**. As said before, categories demonstrate the level of severity which category 1 corresponds to the most and 4 the least severe. In the case of working with TEA, it is essential to keep the solution under a dry inert atmosphere and away from heat. TEA and all its solutions are packed in cylinders and portable tanks. Containers should also be fabricated from carbon steel and be equipped with dip tubes for top discharge, and all connections are located in the vapor space (New Jersey Department of Health and Senior Services, 1996).

***Table 5**. Hazard identification of TEA and its mixture* (GHS, 2017).

Hazards	Category	Hazard statements
Physical hazards		
Flammable liquid	Category 2	H225
Substances/mixture which, in contact with water emit flammable gas	Category 1	H260
Pyrophoric liquid	Category 1	H250
Health hazards		
Skin Corrosion/Irritation	Category 1B	H314
Serious Eye Damage/Eye Irritation	Category 1	H318
Environmental hazards	No data available	

In addition, hazard Statements for triethylaluminium are expressed as follows and clarified with pictograms shown in **Figure 6**:

- H225 - Highly flammable liquid and vapor
- H250 - Catches fire spontaneously if exposed to air
- H260 - In contact with water releases flammable gases which may ignite spontaneously
- H314 - Causes severe skin burns
- H318 - Causes serious eye damage

***Figure 6**. Triethylaluminium pictogram for physical and health hazard* (SDS, Soul, 2021).

The firefighting capabilities of TEA are restricted due to the high radiant heat and the fact that the fire cannot be realistically extinguished because air contact instantly reignites the flames. As a result, firefighters' actions are limited to reducing fire dynamics and radiated heat by cutting off the air supply to the burning area if possible and using water spray to cool nearby facilities. Due to the intense reactivity of aluminum alkyls with water, it must be guaranteed that no water aerosols penetrate the fire and support it at this moment (Heyn, 2015).

Dry extinguishing powders are ideally suited for firefighting and should be applied to the burning surface with applicators if possible. 5 - 10 kg of dry powder per kg of TEA is necessary to provide regulated burn out. Vermiculite can be used as a substitute to dry powder. The light-absorbing substance is especially well-suited to huge fires. In burning trenches and pits, vermiculite-filled plastic sacks are commonly employed. The material spreads over the surface once the sacks melt, reducing the oxygen supply (Heyn, 2015).

3. Theoretical modeling of radiant heat for TEA pool fire

In theoretical modeling, a real-world problem is described in mathematical terms, usually in the form of equations, and then these equations are used both to understand the original problem and to discover new components.

Radiant heat, also known as thermal radiation, is a form of electromagnetic radiation that describes the transfer of energy. Here, for the development of an effective fire protection solution, it is needed first to calculate the heat flux as a function of the size of the fire respectively to the size of the leakage and the distance from the fire. As we are working with a flammable liquid such as TEA, in the case of experiencing an accidental release on the ground or water if it ignites, it will result in a pool fire. **Figure 7** shows different types of pool fires resulting from loss of liquid contaminants. A layer of volatile liquid fuel burns and evaporates in a pool fire. The fuel layers can either be on a horizontal solid substrate or float on a higher density liquid, usually water. The fire safety field is very interested in pool fires since many liquid fuels are stored and transported by different industries (Casal, 2017).

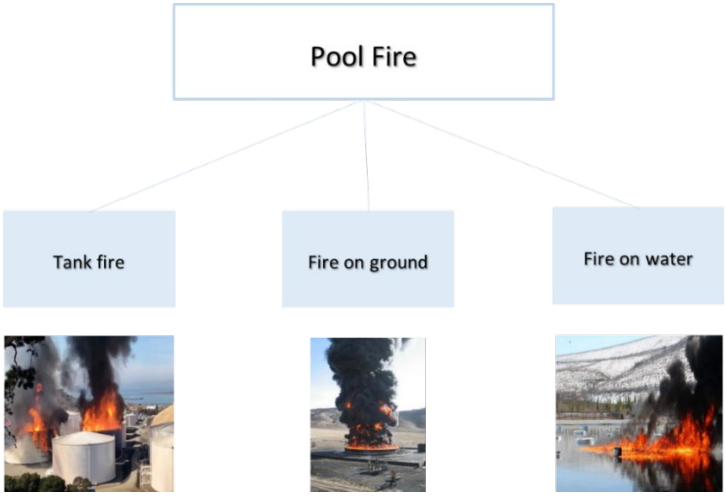

***Figure 7**. Different types of pool fire accident* (Schuessler, 2016).

The radiation heat of TEA pool fire and its solution can be calculated according to the following steps (Heyn, 2015) :

- Determination of the burning rate
- Calculation of the average flame length/height
- Calculation of the flame surface emissive power
- Calculation of atmospheric transmissivity
- Calculation of the view factor
- Calculation of the heat flux

For calculating each step, many different methods and equations have been introduced in the literature; each has its characteristic based on its related parameters.

3.1. Calculation of burning rate

The computation of burning rate is the first step in calculating the consequences of a pool fire, which demonstrates the velocity of consumption of the fuel from the liquid pool. The four most common equations available in the literature are introduced in this section (Bubbico et al., 2016).

3.1.1. **SFPE hand-book** (Morgan J.Hurley, SFPE, 1988)

$$\dot{m}" = A \cdot y' \cdot \rho \qquad \textit{Equation 3}$$

$\dot{m}"$ Fuel mass burning rate (kg·m^{-2}·s^{-1})

A Spill fire area (m^2)

y' Fuel burning regression rate (m·s^{-1}) , is the rate at which the fuel surface descends in a vertical direction as it burns.

ρ Density of the fuel (kg·m^{-3})

3.1.2. **Zabetakis and Burgess equation** (Morgan J.Hurley, SFPE,1988)

$$\dot{m}" = \dot{m}"_{\infty}\left(1 - e^{-k\beta D}\right) \qquad \textit{Equation 4}$$

$$\dot{m}"_{\infty} = 10^{-3}\frac{\Delta H_c}{\Delta H_v{}^*} \qquad \textit{Equation 5}$$

Parameters for Equation 4 should be obtained experimentally for each specific substance.

Where:

$\dot{m}"_{\infty}$ The specific mass burning rate at ''infinite'' diameter (kg·m^{-2}·s^{-1})

k The absorption-extinction coefficient of the flame (m^{-1})

β The correction coefficient for the beam length

D The pool diameter (m)

ΔH_c Heat of combustion (kJ·kg^{-1})

$\Delta H_v{}^*$ Modified heat of vaporization at the boiling point of liquid (kJ·kg^{-1})

3.1.3. **Burgess equation** (Stoffen, yellow book ,1997)

$$\dot{m}" = 1.27 \cdot 10^{-6} \cdot \rho \cdot \frac{\Delta H_c}{\Delta H_v{}^*} \qquad \textit{Equation 6}$$

$$\Delta H_v{}^* = \Delta H_v + \int_{T_a}^{T_b} C_p dT \qquad \textit{Equation 7}$$

Where:

ΔHv Heat of vaporization (kJ·kg^{-1})

C_p Specific heat capacity of the liquid

T_b Boiling temperature (ºC)

T_a Ambient temperature, 25 (ºC)

3.1.4. **Mudan equation** (Morgan J.Hurley, SFPE,1988)

$$\dot{m}" = 1.10^{-3} \frac{\Delta H_c}{\Delta H_v{}^*} \qquad \textit{Equation 8}$$

Where:

$\Delta H_v{}^*$ Modified heat of vaporization at the boiling point of liquid (kJ·kg^{-1})

ΔHc Heat of combustion (KJ·kg^{-1})

3.2. Calculation of the average flame length

The flame height is a critical parameter in determining the effects and behavior of a pool fire, and several models have been offered for its quantification throughout the years, some of which are described here (Bubbico et al., 2016).

3.2.1. Heskestad equation (Morgan J.Hurley, SFPE, 1988)

$$L_f = 0.23\, Q_r^{\frac{2}{5}} - 1.02D \qquad \textit{Equation 9}$$

$$Q_r = A \cdot \dot{m}''_{\infty} \cdot \Delta H_c \qquad \textit{Equation 10}$$

Where:

- L_f The 50-percentile intermittent flame height (m)
- D The diameter of the fire (m)
- Q_r The heat release rate (kW)

3.2.2. Thomas equation (Morgan J.Hurley, SFPE, 1988)

$$\frac{H}{D} = 42\left(\frac{\dot{m}''}{\rho_a\sqrt{gD}}\right)^{0.61} \qquad \textit{Equation 11}$$

Where:

- H Average flame length (m)
- D The diameter of pool fire (m)
- $\dot{m}''$ Mass burning rate per unit pool area ($kg \cdot m^{-2} \cdot s^{-1}$)
- ρ_a Ambient air density, 1.225 ($kg \cdot m^{-3}$)
- g Gravitational acceleration, 9.8 ($m \cdot s^{-2}$)

3.2.3. **Zhang et al. equation** (Bubbico et al., 2016)

$$\frac{H}{D} = 1.73 + 0.33D^{-1.43} \qquad \textit{Equation 12}$$

Where:

D The diameter of pool fire (m)

3.3. Calculation of the flame surface emissive power

The radiant heat emitted per unit surface of the flame and per unit time is referred to as emissive power. It represents the fire's radiative characteristics. In fact, the thermal radiation of the flame is generated by the fire's entire volume, not only its surface. The introduced equations here can be used to express emissive power (Casal, 2017).

3.3.1. **Burgess and Hertzberg equation** (Stoffen, yellow book ,1997)

$$SEP_{max} = \frac{F_s \cdot \dot{m}'' \cdot \Delta H_c}{\left(1 + 4 \cdot \frac{L}{D}\right)} \qquad \text{Equation 13}$$

Where:

SEP_{max} Maximum Surface Emissive Power from a flame without soot production in ($J \cdot m^{-2} \cdot s^{-1}$)

F_s Fraction of the combustion energy radiated from the flame surface; according to Burgess, Hertzberg [1974], is independent from D between 0.1–0.4.

$\dot{m}''$ Burning rate at still weather conditions in ($kg \cdot m^{-2} s^{-1}$)

ΔH_c Heat of combustion in ($J \cdot kg^{-1}$)

L Average flame height (m)

D Pool diameter (m)

3.3.2. **Shokri and Beyler equation** (Morgan J.Hurley, SFPE, 1988)

$$E = 58(10^{-0.00823D}) \qquad \textit{Equation 14}$$

Where:

E Equivalent emissive power (kW·m^{-2})

D The pool fire diameter(m)

This represents the average emissive power over the whole of the flame and is significantly less than the emissive powers that can be attained locally.

3.3.3. **Mudan method** (Morgan J.Hurley, SFPE, 1988)

$$E = E_{max}e^{-sD} + E_s[1 - e^{-sD}] \qquad \textit{Equation 15}$$

Where:

E_{max} Equivalent blackbody emissive power, 140 (kW·m^{-2})

s Extinction coefficient, 0.12 (m^{-1})

D Equivalent pool diameter (m)

E_s Emissive power of smoke, 20 (kW·m^{-2})

3.3.4. **Point source model** (Stoffen, yellow book, 1997)

$$E = \sigma\varepsilon\left(T_{fl}^4 - T_a^4\right) \qquad \textit{Equation 16}$$

Where:

σ The Stefan-Boltzmann constant, 5.6704×10^{-8} (W·m^{-2}·K^{-4})

ε The emissivity, which depends on the substance present in the flame (value between 0 and 1)

T_{fl} The radiation temperature of the flame (significantly lower than the adiabatic flame temperature) (K). The flame temperature of 1400 K was considered in SFPE hand-book (Morgan J.Hurley, 1988)

T_a The ambient temperature, 298 (K)

3.3.5. **Solid flame model** (Stoffen, yellow book, 1997)

$$E = \frac{\eta_{rad} \cdot \dot{m}'' \cdot \Delta H_c}{A} \qquad \textit{Equation 17}$$

$$\eta_{rad} = 0.35e^{-0.05D} \qquad \textit{Equation 18}$$

Where:

$\dot{m}''$ The burning rate (kg·s^{-1})

ΔH_c Heat of combustion (kJ·kg^{-1})

η_{rad} The radiative fraction or radiant heat fraction

A The area of the solid flame from which radiation is released (m^2)

D The pool fire diameter (m)

3.4. Calculation of atmospheric transmissivity

The absorption of heat radiation by the atmosphere, primarily by carbon dioxide and water vapor, is measured by atmospheric transmissivity. This absorption reduces the amount of radiation that reaches the target surface. The distance between the flames and the target determines the atmospheric transmissivity. While the amount of carbon dioxide in the atmosphere remains relatively constant, water vapor in the atmosphere is affected by temperature and humidity. Formulas for calculating atmospheric transmissivity are provided below (Casal, 2017).

3.4.1. **Transmissivity model** (Stoffen, yellow book, 1997)

$$\tau = 1.53\left(p_w . d\right)^{-0.06} \quad for\ p_w . d < 10^4\ \frac{N}{m} \qquad \textit{Equation 19}$$

$$\tau = 2.02\left(p_w \cdot d\right)^{-0.09} \quad for\ 10^4 \ll p_w \cdot d \ll 10^5\ \frac{N}{m} \qquad \textit{Equation 20}$$

$$\tau = 2.85\left(p_w \cdot d\right)^{-0.12} \quad for\ p_w \cdot d > 10^5\ \frac{N}{m} \qquad \textit{Equation 21}$$

$$p_w = p_{wa}\ \frac{H_R}{100} \qquad \textit{Equation 22}$$

$$\ln p_{wa} = 23.18986 - \frac{3816.42}{(T_a - 46.13)} \qquad \textit{Equation 23}$$

Where:

τ	The atmospheric transmissivity
d	The distance between the surface of the flame and the target (m)
p_w	The partial pressure of water in the atmosphere ($N \cdot m^{-2}$)
H_R	The relative humidity of the atmosphere (%)
p_{wa}	The saturated water vapor pressure at the atmospheric temperature ($N \cdot m^{-2}$)
T_a	The ambient temperature, 298 (K)

3.5. Calculation of the view factor for vertical cylinder

The view factor is the ratio between the amount of thermal radiation released by a flame and the amount of thermal radiation received by an object, not in contact with the flame. It appears in all thermal radiation calculations. This ratio, which is seen in this part can be affected by the shape and size of the fire, the distance between the flame and the receiving element, and the relative position of the flame and the target surfaces (Casal, 2017).

3.5.1. **Shokri and Beyler** (Morgan J.Hurley, SFPE, 1988)

$$F_{max} = \sqrt{F_H^2 + F_V^2} \qquad \textit{Equation 24}$$

$$F_H = \frac{B - \frac{1}{S}}{\pi\sqrt{B^2 - 1}} \tan^{-1}\sqrt{\frac{(B+1)(S-1)}{(B-1)(S+1)}} - \frac{(A - \frac{1}{S})}{\pi\sqrt{A^2 - 1}}\tan^{-1}\sqrt{\frac{(A+1)(S-1)}{(A-1)(S+1)}} \qquad \textit{Equation 25}$$

$$F_V = \frac{1}{\pi S}\tan^{-1}\left(\frac{h}{\sqrt{S^2 - 1}}\right) - \frac{h}{\pi S}\tan^{-1}\sqrt{\frac{S-1}{S+1}} + \frac{Ah}{\pi S\sqrt{A^2 - 1}}\tan^{-1}\sqrt{\frac{(A+1)(S-1)}{(A-1)(S+1)}} \qquad \textit{Equation 26}$$

$$A = \frac{h^2 + S^2 + 1}{2S} \qquad \textit{Equation 27}$$

$$B = \frac{1 + S^2}{2S} \qquad \textit{Equation 28}$$

$$S = \frac{2L}{D} \qquad \textit{Equation 29}$$

$$h = \frac{2H}{D} \qquad \textit{Equation 30}$$

Where:

L	Distance between the center of the cylinder to the target (m)
H	Height of the cylinder (m)
D	Cylinder diameter (m)
F_H	Horizontal view factor
F_V	Vertical view factor

F_{max} Maximum view factor

3.5.2. **Point source model** (Stoffen, yellow book, 1997)

$$F_{max} = \sqrt{F_H^2 + F_V^2}$$ *Equation 31*

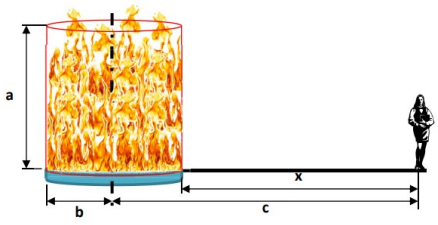

***Figure 8**. The solid flame models*

Table 6 and **Table 7** can be used in order to obtain F_H and F_v:

***Table 6**. Vertical view factor **(F_v)** for a cylindrical fire.*

	Vertical view factor (F_v)				a/b					
c/b	0,1	0,2	0,5	1,0	2,0	3,0	5,0	6,0	10,0	20,0
1,10	0,330	0,415	0,449	0,453	0,454	0,454	0,454	0,454	0,454	0,454
1,20	0,196	0,308	0,397	0,413	0,416	0,416	0,416	0,416	0,416	0,416
1,30	0,130	0,227	0,344	0,376	0,383	0,384	0,384	0,384	0,384	0,384
1,40	0,096	0,173	0,296	0,342	0,354	0,356	0,356	0,357	0,357	0,357
1,50	0,071	0,135	0,253	0,312	0,329	0,312	0,333	0,333	0,333	0,333
2,00	0,028	0,056	0,126	0,194	0,236	0,245	0,248	0,249	0,249	0,249
3,00	0,009	0,019	0,047	0,086	0,132	0,150	0,161	0,163	0,165	0,166
4,00	0,005	0,010	0,024	0,047	0,080	0,100	0,115	0,119	0,123	0,124
5,00	0,003	0,006	0,015	0,029	0,053	0,069	0,086	0,091	0,097	0,099
10,00	0,000	0,001	0,003	0,006	0,013	0,019	0,029	0,032	0,042	0,048
20,00	0,000	0,000	0,000	0,001	0,003	0,004	0,007	0,009	0,014	0,020
50,00	0,000	0,000	0,000	0,000	0,000	0,000	0,001	0,001	0,002	0,004

***Table 7**. Horizontal view factor **(F_h)** for a cylindrical fire.*

	Horizontal view factor (F_h)				a/b					
c/b	0,1	0,2	0,5	1,0	2,0	3,0	5,0	6,0	10,0	20,0
1,10	0,132	0,242	0,332	0,354	0,360	0,362	0,362	0,362	0,363	0,363
1,20	0,044	0,120	0,243	0,291	0,307	0,310	0,312	0,312	0,313	0,313
1,30	0,020	0,065	0,178	0,242	0,268	0,274	0,277	0,270	0,278	0,279
1,40	0,011	0,038	0,130	0,203	0,238	0,246	0,250	0,251	0,252	0,253
1,50	0,005	0,024	0,097	0,170	0,212	0,222	0,228	0,229	0,231	0,232
2,00	0,001	0,005	0,027	0,073	0,126	0,145	0,158	0,160	0,164	0,166
3,00	0,000	0,000	0,005	0,019	0,050	0,071	0,091	0,095	0,103	0,106
4,00	0,000	0,000	0,001	0,007	0,022	0,038	0,057	0,062	0,073	0,078
5,00	0,000	0,000	0,000	0,003	0,011	0,021	0,037	0,043	0,054	0,061
10,00	0,000	0,000	0,000	0,000	0,001	0,003	0,007	0,009	0,017	0,026
20,00	0,000	0,000	0,000	0,000	0,000	0,000	0,001	0,001	0,003	0,003
50,00	0,000	0,000	0,000	0,000	0,000	0,000	0,000	0,000	0,000	0,000

3.6. Calculation of the heat flux

3.6.1. **Mudan method** (Morgan J.Hurley, SFPE, 1988)

$$Q'' = E \cdot F_{max} \cdot \tau_a \qquad \textit{Equation 32}$$

Where:

Q''	Heat flux of pool fire (kW·m^{-2})
E	Average emissive power at flame surface (kW·m^{-2})
F_{max}	Maximum geometrical view factor of the radiated object
τ_a	Atmospheric transmissivity

3.6.2. **Shokri and Beyler equation** (Morgan J.Hurley, SFPE, 1988)

$$Q'' = 15.4\left(\frac{L}{D}\right)^{-1.59} \qquad \textit{Equation 33}$$

L	The distance from the center of the pool fire to the target edge
D	The diameter of pool fire (m)
A	The surface area of the noncircular pool (m^2)

3.6.3. **Point source model** (Stoffen, yellow book, 1997)

$$I = \frac{Q_r}{4\pi l_p^2} \quad or \quad I = \frac{\eta_{rad}\, \dot{m}''\Delta H_c\, \tau\, \cos\varphi}{4\pi\, l_p^2} \qquad \textit{Equation 34}$$

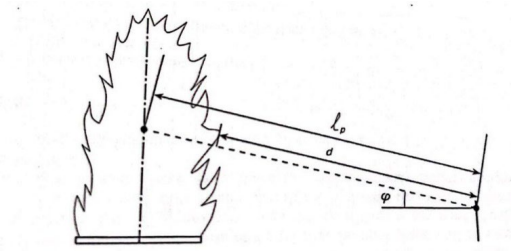

Figure 9 *. The point source model.*

I The thermal radiation intensity (kW·m^{-2})

l_p The distance between the point source and the target (m)

φ The angel between the plane perpendicular to the receiving surface and the line joining the source point and the target (°)

τ The atmospheric transmissivity

$\dot{m}''$ The burning rate (kg·s^{-1})

ΔH_c Heat of combustion (kJ·kg^{-1})

Q_r The heat released as thermal radiation per unit time (kW)

η_{rad} The radiative fraction or radiant heat fraction

D The pool fire diameter (m)

4. Experimental data on TEA pool fires

In this chapter data gathered on TEA burning behavior is presented. Data includes TEA thermal properties as well as fire metrics, as those included in the equations reported in **Chapter 3.** Data has been extracted from pool fire experiments found in the literature.

4.1. Burning rate data

TEA and isopentane thermal properties are gathered in **Table 8**:

Table 8*. TEA and isopentane thermal properties* (Glo-En, 2021)

Product	ΔHc **(kJ kg^{-1})**	ΔHv **(J g^{-1})**	Cp **(J g^{-1} ◦C^{-1})**	T_b **(ºC)**	ρ **(kg m^{-3})**	M_w **(g mol^{-1})**
TEA	-44694	536	2.23	186	832	114.2
Isopentane	-48532	342	2.28	28	616	72.2

An aluminum alkyl solution is usually a mixture of an inert solvent with an aluminum alkyl. The burning rate of the mixture is determined by the evaporation of the two components in the combustion zone. Due to their different volatilities, the burning rate of the solvent is much higher than that of the aluminum alkyl, which it has been shown concerning TEA and its solution in **Table 9**. Fire tests of AkzoNobel confirmed this phenomenon (AkzoNobel, 2008). According to the experimental data, TEA solutions show a maximum burning rate at the beginning, which decreases continuously with the increasing duration of the fire (Heyn, 2015). According to the experimental data gathered in **Table 9,** the maximum burning rate of 0.083 (kg·m^{-2}·s^{-1}) was achieved in an 11% TEA solution in isopentane.

Table 9*.Mass burning rate per unit area versus the thermochemical property of fuels burning as pool fires* (AkzoNobel, 2008)*.*

Product	$\dot{m}''$ **(kg m^{-2} s^{-1})**
Neat TEA	0.056
11%TEA/Isopentane	0.083-0.033
22%TEA/Isopentane	0.078-0.030
20%TEA/n-Hexane	0.073-0.037
50%TEA/n-Hexane	0.072-0.037

4.2. Flame height data

The flame height of the TEA and its solution with isopentane have been experimentally measured by (AkzoNobel, 2008) and collected in **Table 10**. It has been observed that adding solvent to TEA will result in a higher flame height. These measurements were all obtained for the pool fire of 1 m^2, and it has been experienced as it can be observed in **Table 11** that increasing the pool fire area will affect the rising flame height (AkzoNobel, 2008).

***Table 10**. Measured flame heights for **1 m^2** pool fire* (AkzoNobel, 2008).

Product	Flame height (m)
TEA	2
Isopentane	4
N-Hexane	3.1
TEA solution	> 2

***Table 11**. Flame heights of neat TEA and hydrocarbon solvent pool fires for larger surfaces* (AkzoNobel, 2008).

Product	Flame heights (m) with pool surface of		
	5 m^2	**10 m^2**	**15 m^2**
TEA	4	5	6
Isopentane	8	10	12
N-Hexane	6.5	8	10

4.3. Emissive power data

According to the energy distribution, the average emissive power of the non-luminous component of the flame is E_{soot}=40 $kW \cdot m^{-2}$, and this value is independent of the pool diameter or the type of fuel. Depending on fuel and pool diameter, the luminous zone's typical emissive power is E_{lum} = 80–120 $kW \cdot m^{-2}$. The overall average value of E was found to increase as a function of diameter up to approximately 5 m. According to different experiments, the overall emissive power decreases with larger diameters (Muñoz et al., 2007).

The predicted values are significantly higher than the experimental ones. In fact, the existing models overpredict the value of E for pool fires with diameters of up to 10m and give relatively low values for large pool fires (more than 20m in diameter) (Muñoz et al., 2007).

4.4. Heat flux data

Table 12 represents the changing behavior of flame temperature and heat flux at the distance of 24 meters from the fire at different burning times. As it was expected thermal radiation and temperature followed a same trend. It has been observed from experiments that the thermal radiation and temperature received to a target at 24 meters far from the isopentane and TEA solution fire is much higher than that from the neat TEA fire (AkzoNobel, 2008).

The maximum heat flux of 270 ($W \cdot m^{-2}$) and flame temperature of 1400 K in **Table 12** corresponds to isopentane after 60 seconds of burning. Based on the gathered experimental data, during the first 140 seconds of burning, the thermal intensity and temperature of 22%TEA/Isopentane at the distance of 24m will reach its maximum amount of 200 ($W \cdot m^{-2}$) and 1300 (K). In the middle duration (140-240 s), both parameters decrease gradually, and after 240 seconds, the thermal radiation and flame temperature will get constant at 50 ($W \cdot m^{-2}$) and 1150 K, similar to neat TEA radiation (AkzoNobel, 2008).

As a result, adding solvent to TEA can increase the flame temperature, thermal radiation, and the intensity of the solution, which reached its maximum of 200($W \cdot m^{-2}$) and 1300 (K) after 140s. Concerning the neat TEA intensity, the maximum radiation of 50 ($W \cdot m^{-2}$) and maximum temperature of 1150 (K) have been achieved at the distance of 24 meters after 30 s (AkzoNobel, 2008).

***Table 12**. The measured thermal intensity and temperature **(24 meters from the fire)** versus the burning time* (AkzoNobel, 2008).

	Burning time (s)	Thermal radiation (W m^{-2})	Temperature (K)
TEA	>30	50	1150
Isopentane	>60	270	1400
22%TEA/Isopentane	0-140	200	1300
	140-240	200-50	1300-1150
	>240	50	1150

The results of a 1 m^2 pool fire from burning experiments were used by (AkzoNobel, 2008) to measure radiation intensities of large fires at different distances from center of fire. As observed in

Table 13, measured radiation intensity decreased by increasing the distance from the center of the pool fire, so the maximum radiation (20 $kW \cdot m^{-2}$) for neat TEA , (40 $kW \cdot m^{-2}$) for n-hexane and (45 $kW \cdot m^{-2}$) for isopentane obtained in the minimum distance of 2 m. In addition, it has been experienced that all the substances will reach zero thermal radiation at approximately 15 meters from the center of the fire (AkzoNobel, 2008).

Table 13**.Relation between the thermal intensity and the distance from center of the fire for pool area of **1 m^2 (AkzoNobel, 2008).

	Thermal radiation ($kW\ m^{-2}$) at the distances of		
	2 (m)	**5 (m)**	**15 (m)**
TEA	20	3	0
N-Hexane	40	6	0
Isopentane	45	10	0

In **Table 14** and **Table 15** almost same behavior was obtained for pool fire with the surface area of 5 m^2 and 10 m^2. In the case of increasing the pool area, zero radiation intensity was achieved at further distances. For a 5 m^2 TEA pool fire, zero thermal radiation was achieved at a distance of 20 m, but at a distance of 30 m for a 10 m^2 pool fire. The same pattern has been attained with isopentane and n-hexane at the distance of 30 m shifted to 40 m (AkzoNobel, 2008).

Table 14**. Relation between the thermal intensity and the distance from center of the fire for pool area of **5 m^2 (AkzoNobel 2008).

	Thermal radiation ($kW\ m^{-2}$) at the distances of			
	2 (m)	**5 (m)**	**15 (m)**	**20 (m)**
TEA	43	12	1	0
N-Hexane	>50	40	3	1
Isopentane	>50	50	4	3

Table 15**. Relation between the thermal intensity and the distance from center of the fire for pool area of **10 m^2 (AkzoNobel 2008).

	Thermal radiation ($kW\ m^{-2}$) at the distances of			
	2 (m)	**5 (m)**	**15 (m)**	**30 (m)**
TEA	>50	30	2	0
N-Hexane	>50	47	5	1
Isopentane	>50	>50	9	3

When the thermal intensity emitted by burning fuel is known as a function of distance, the thermal radiation damage levels can be used to calculate safe distances for people, equipment, and buildings. For 1, 5, and 10 m^2 pool fires of neat TEA and isopentane, the distance from the fire where the thermal radiation received correlates with the thermal radiation damage levels is provided in **Table 16** and **Table 17**. The data shows the distances that must be considered to minimize the thermal radiation harm to personnel (pain or injury) and equipment (mechanical integrity).

Personnel not wearing any protective clothing, should stay at least 9, 14, 18 meters away from respectively a 1, 5, 10 m^2 pool fire of neat TEA. In case of an isopentane fire personnel should at least stay twice as far away from the pool fire.

Building and equipment safety distances are quite short, which implies that actual thermal radiation damage will only occur when structures or equipment are extremely close to the fire and exposed for an extended length of time.

***Table 16**. The distances from a 1, 5and 10 m^2 **neat TEA** pool fire where the thermal radiation received corresponds with the thermal radiation damage levels for personnel and equipment* (AkzoNobel, 2008).

Thermal radiation damage levels(kW m^{-2})	**Effect on personnel and equipment**	**Distance (m) from pool fire with surface of**		
		1 m^2	**5 m^2**	**10 m^2**
1	Personnel: Highest heat flux on skin during long period without feeling pain	9	14	18
2.1	Personnel: Minimum value to be felt as pain after 1 minute exposure of skin	7.5	10	14
4.7	Personnel: Pain after 15-20 seconds exposure and injury after 30 seconds	4.5	8.5	10
12.6	Building: Exposed wood and flammable vapors could be ignited	3.5	5	8
23	Tanks, equipment: Thin, uninsulated steel can lose mechanical integrity	1.8	4	6

Table 17. *The distances from a 1, 5 and 10 m² **isopentane** pool fire where the thermal radiation received corresponds with the thermal radiation damage levels for personnel and equipment* (AkzoNobel, 2008).

Thermal radiation damage levels(kW m^{-2})	Effect on personnel and equipment	Distance (m) from pool fire with surface of		
		1 m^2	**5 m^2**	**10 m^2**
1	Personnel: Highest heat flux on skin during long period without feeling pain	14	28	36
2.1	Personnel: Minimum value to be felt as pain after 1 minute exposure of skin	9.5	19	28
4.7	Personnel: Pain after 15-20 seconds exposure and injury after 30 seconds	7.5	14.5	18
12.6	Building: Exposed wood and flammable vapors could be ignited	4.5	9.5	13.5
23	Tanks, equipment: Thin, uninsulated steel can lose mechanical integrity	4	8	10.5

5. Pool fire modeling

In **Chapter 5**, a pool fire scenario containing a TEA substance will be developed to examine its thermal behavior and compare it to experimental data acquired from the literature in **Chapter 4**. Another purpose of this chapter is to examine and contrast the precision of the various models and equations established in **Chapter 3**.

To compare the diverse models, a hypothetical scenario has been defined. **Figure 10** shows a scheme of the scenario consisting on a TEA pool fire with a diameter of 5 meters resulted from a tank leakage in an industrial facility. The relative humidity is considered to be 45 %, the temperature is 25 °C, and there will be no wind. The maximum heat radiation at the horizontal distances of 2, 5, and 20 meters from the flame tip will be computed.

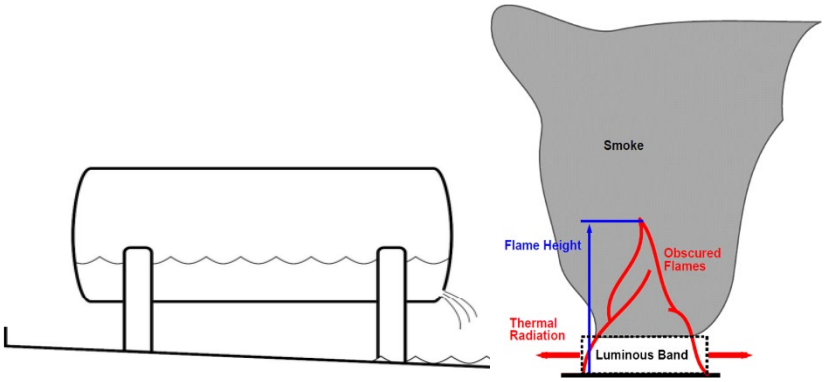

***Figure 10**. TEA leakage from tank resulted in a pool fire* (Casal, 2017).

5.1. Neat TEA

5.1.1. TEA burning rate computation

The burning rate of TEA was calculated using input data from **Table 8** with various correlations.

The literature has presented experimental data for regression rate (y') of TEA (AkzoNobel, 2008). The most commonly referenced database was developed for pool fires and presented in SFPE handbook, which shows the regression rate and flame height results for various fuels burning in a broad range of pool sizes, 0.004–23 m in diameter. The data indicated that the fuel regression rate is approximately constant at 4 mm·min^{-1} for all fuels tested burning as confined pool fires with diameters greater than 1 m (Morgan J.Hurley, SFPE, 1988). The maximum burning rate of 0.044 (kg·m^{-2}·s^{-1}), was calculated with **Equation 3** for TEA which was lower but close to other results.

Mudan equation with a mass flux of 0.050 ($kg \cdot m^{-2} \cdot s^{-1}$) matched with other correlations. Compared to **Equation 3** the Mudan equation is preferable and does cover a broader range of fuels, including liquefied gases (Morgan J.Hurley, SFPE, 1988).

For calculating with Zabetakis and Burgess equation, since the defined pool fire scenario has a large diameter, the maximum mass burning rate will be considered equal to infinite burning rate of 0.053 ($kg \cdot m^{-2} \cdot s^{-1}$).

The burning rate of TEA has been computed as 0.053 ($kg \cdot m^{-2} \cdot s^{-1}$) with **Equation 6**. It was recommended, if the burning rate was not measured experimentally, the Burgess equation could be the best correlation to predict the burning rate of a combustible liquid (single component) under ambient conditions (Morgan J.Hurley, SFPE, 1988). The calculated values are close and fit with the experimental data of 0.056 ($kg \cdot m^{-2} \cdot s^{-1}$) in **Table 9**.

The burning rate of **0.053 ($kg \cdot m^{-2} \cdot s^{-1}$)** from **Table 18** was selected for further calculations.

***Table 18**. The burning rate of **TEA** with 5 m diameter pool fire.*

Correlation number	Correlation reference	Equation	Burning rate ($kg\ m^2\ s^{-1}$)
1	Regression model	Equation 3	**0.044**
2	Zabetakis and Burgess	Equation 4	**0.053**
3	Burgess equation	Equation 6	**0.053**
4	Mudan equation	Equation 8	**0.050**

5.1.2. TEA flame height computation

The burning rate of 0.053 ($kg \cdot m^{-2} \cdot s^{-1}$) was used in order to calculate the average flame height of 5 diameters pool fire of TEA. The results were produced by using various correlations in **Table 19**. Based on **Table 11**, average flame height of approximately 7 m was predicted for a pool fire with diameter of 5 and accordingly the area of 20 m^2. The computed results are close to expected value and acceptable. Obtaining slightly over calculated flame height has been estimated by AkzoNobel (AkzoNobel, 2008).

The differences in results are due to the fact that each correlation uses distinct dependencies and parameters. In Heskestad correlation, the height of the flame is dependent on the heat produced by the fire, instead of the burning rate used in Thomas equation. In Zhang et al. equation even simpler approach has been introduced, since the height of the flame is only dependent on the diameter of the pool. Among all, the Thomas correlation is the most well-known and extensively used for estimating

the ratio between the flame height and the diameter of a circular pool (Bubbico, Dusserre, and Mazzarotta, 2016).

The average height of **10 meters** which also matched with Thomas correlation has been considered for following calculations.

Table 19. *The average flame height of* ***TEA*** *with 5 m diameter pool fire.*

Correlation number	Correlation reference	Equation	Average flame height (m)
1	Heskestad equation	Equation 9	**11**
2	Thomas equation	Equation 11	**10**
3	Zhang et al. equation	Equation 12	**9**

5.1.3. TEA emissive power computation

Following, the emissive power of TEA flames has been computed and compared in **Table 20**. Results of emissive power are around 50 ($kW \cdot m^{-2}$) excepting the result of 86 ($kW \cdot m^{-2}$) which corresponds to Mudan equation. Based on the SFPE book, Mudan equation over-predicts emissive power for pool fire diameters less than 15 meters (Morgan J.Hurley, SFPE, 1988).

Both Shokri and Beyler and the method of Mudan use an emissive power averaged over the flame height of the fire. Both correlations fall below 31.5 ($kW \cdot m^{-2}$) for fires larger than 30 diameters. These correlations can wrongly be interpreted to mean that buildings can be built right next to sites of potentially large fires simply because the predicted flux would never exceed 31.5 ($kW \cdot m^{-2}$) regardless of its distance from the fire (McGrattan et al., 2000).

Burgess and Hertzberg correlation has been suggested for the surface emissive power which will be greatly reduced by the formation of soot (Heyn, 2015). The emissive power of **53 ($kW \cdot m^{-2}$)** has been chosen for the following calculations.

Table 20*. The emissive power of* ***TEA*** *with 5 m diameter pool fire.*

Correlation number	Correlation reference	Equation	Emissive power ($kW\ m^{-2}$)
1	Burgess and Hertzberg	Equation 13	53
2	Shokri and Bayer	Equation 14	53
3	Mudan equation	Equation 15	86
4	Point source model	Equation 16	54
5	Solid flame model	Equation 17	43

5.1.4. Transmissivity computation

The transmissivity of TEA in condition of 45% relative humidity has been calculated in **Table 21** for different horizontal distances of 2, 5 and 20 meters from the fire flame. As expected, as the distance between the transmitter and the receiver increased, the transmissivity decreased from **0.98 to 0.83**.

Table 21. The transmissivity of **TEA** with 5 m diameter pool fire for different distances from target.

Correlation number	Correlation reference	Equation	transmissivity		
			2 m	5 m	20 m
1	Transmissivity model	Equation 19, 20, 21	0.98	0.91	0.83

5.1.5. TEA maximum view factor computation

The maximum configuration factors of TEA at the target locations of 2, 5 and 20 meters are determined using Shokri and Beyler equation and point source model in **Table 22**. Both correlations yielded about the same maximum view factor, so the point source model was chosen for the following calculations, which ranges from **0.35 to 0.05**.

Table 22. *The maximum view factor of **TEA** and different distances from target with 5 m diameter pool fire.*

Correlation number	Correlation reference	Equation	Maximum view factor		
			2 m	5 m	20 m
1	Shokri and Beyler	Equation 24	0.31	0.19	0.03
2	Point source model	Equation 31	0.35	0.18	0.05

5.1.6. TEA heat flux computation

All the required parameters which were calculated in **Chapter 5** have been used as input in order to calculate the heat radiation in **Table 23**. Different correlations have been introduced in distances of 2, 5, 20 meters to compare the results. Approximately same trend and results have been observed for all the methods. The maximum radiation was attained in the closest target (2 m), as expected, and the fire intensity dropped to near zero at a further distance (20 m).

For radiations less than 5 ($kW \cdot m^{-2}$), the SFPE handbook recommends using the point source model, while the Shokri and Beyler equation and Mudan technique can be used for all flux ranges (Morgan J.Hurley, SFPE, 1988). Also, it is suggested that the Shokri and Beyler model and the point source model are the favored models due to their conservative character and the minimizing of differences between the data and the experiments. Shokri and Beyler can exhibit the best correlation in **Table 23** based on the facts that were presented, which shows a heat flux reduction of **18 to 1 ($kW \cdot m^{-2}$)** for distances of 2 to 20 meters.

The calculated values are slightly lower than the experimental results, but they are acceptable and comparable. Since there is no specific information about the model of sensors and the place where they were located in experiment, view factor can be the main reason which can justify the difference between the experimental and computed values.

According to the values in **Table 16**, personnel not wearing protective clothes should stay at least 25 meters away from a TEA pool fire with a diameter of 5. Skin pain and injury can be noticed at a distance of 2 meters from the fire flame, and tanks and equipment composed of thin, uninsulated steel can lose their mechanical integrity.

Table 23. *The heat flux of* ***TEA*** *at different distances from target with 5 m diameter pool fire.*

Correlation number	Correlation reference	Equation	Heat flux ($kW\ m^{-2}$)		
			2 m	5 m	20 m
1	Mudan method	Equation 32	19	9	2
2	Shokri and Beyler	Equation 33	18	8	1
3	Point source model	Equation 34	19	12	3

5.2. TEA solution

Because multiple TEA solutions are routinely used in industry in addition to neat TEA, it was chosen to repeat all of the computing processes for TEA solution to obtain its thermal behavior. The thermal behavior of **11%TEA/Isopentane** has piqued this thesis's curiosity since, according to **Table 9**, it can reach a high maximum burning rate of 0.083 ($kg \cdot m^{-2} \cdot s^{-1}$). Thermal properties of pure TEA and isopentane in **Table 9** have been used in the combination of 11% of TEA and 79% of isopentane to obtain **Table 24** for 11%TEA/isopentane thermal properties.

***Table 24. 11%TEA/isopentane** thermal properties.*

Product	ΔHc (kJ kg^{-1})	ΔHv (J g^{-1})	Cp (J g^{-1} ◦C^{-1})	T_b (ºC)	ρ (kg m^{-3})	M_w (g mol^{-1})
11%TEA/Isopentane	-48110	363	2.26	107	640	76.8

5.2.1. TEA solution burning rate computation

Same trend for TEA solution has been repeated with lower results in Regression model and Mudan equation in **Table 25**. All the results approximately fit the range of mass flux which was presented in **Table 9** between 0.033 to 0.083 ($kg \cdot m^{-2} \cdot s^{-1}$). Burgess equation with the maximum burning rate of **0.087 ($kg \cdot m^{-2} \cdot s^{-1}$)** have been considered for rest of calculation.

***Table 25**. The burning rate of **11%TEA/Isopentane** with 5 m diameter pool fire.*

Correlation number	Correlation reference	Equation	Burning rate (kg m^{-2} s^{-1})
1	Regression model	Equation 3	0.034
2	Zabetakis and Burgess	Equation 4	0.087
3	Burgess equation	Equation 6	0.087
4	Mudan equation	Equation 8	0.070

5.2.2. TEA solution flame height computation

Based on experimental data on **Table 10**, it was expected to obtain higher flame height in TEA solution compared to pure one. The result of Zhang et al. equation for both TEA and its solution is the same amount since it is just dependent on pool diameter which for both are considered 5 m.

In addition, according to available data in **Table 11**, flame height corresponds to neat isopentane is double of neat TEA. So, the **average height of 13** m for 11%TEA/Isopentane can be obtained which also matches the Thomas equation as the best correlation in **Table 26**.

***Table 26**. The average flame height of **11%TEA/Isopentane** with 5 m diameter pool fire.*

Correlation number	Correlation reference	Equation	Average flame height (m)
1	Heskestad equation	Equation 9	16
2	Thomas equation	Equation 11	13
3	Zhang et al. equation	Equation 12	9

5.2.3. TEA solution emissive power computation

Emissive power has been computed with 5 different correlations in **Table 27**. Values for Shokri and Beyler and Mudan equations were same as neat TEA since pool fire diameter was the only variable. All other correlations have resulted to roughly same value. Based on the Burgess and Hertzberg correlation emissive power of **73 (kW·m^{-2})** has been selected to continue the computation.

***Table 27.** The emissive power of **11%TEA/Isopentane** with 5 m diameter pool fire.*

Correlation number	Correlation reference	Equation	Emissive power (kW m^{-2})
1	Burgess and Hertzberg	Equation 13	73
2	Shokri and Beyler	Equation 14	53
3	Mudan equation	Equation 15	86
4	Point source model	Equation 16	76
5	Solid flame model	Equation 17	75

5.2.4. TEA solution maximum view factor computation

In **Table 28**, the maximum view factor was about the same for both methods. The point source model has been considered for further calculations.

Table 28. *The maximum view factor of* ***11%TEA/Isopentane*** *and different distances from target with 5 m diameter pool fire.*

Correlation number	Correlation reference	Equation	Maximum view factor		
			2 m	5 m	20 m
1	Shokri and Beyler	Equation 24	0.27	0.21	0.02
2	Point source model	Equation 31	0.30	0.19	0.04

5.2.5. TEA solution heat flux computation

All the computed values in green in previous tables have been used to calculate the heat flux of TEA solution in **Table 29**. The similar condition and case study was defined and repeated for TEA solution. As a result, the same transmissivity in **Table 21** was used for TEA solution.

The only factors that vary in the Shokri and Beyler approach are the distance from the flame and the pool fire diameter. Therefore, the obtained results for 11%TEA/Isopentane were same as TEA with **Equation 32.** Point source model has been recommended as the preferred model for all the thermal intensity ranges.

Based on the data presented in **Table 16** and **Table 17**, an individual who does not wear protective clothing must stay at least 35 meters away from a TEA pool fire with a diameter of five meters. In addition to skin pain and injury, flammable vapors and wood are at risk of ignition when they are within 5 m of the flame.

Table 29*. The heat flux of* ***11%TEA/Isopentane*** *at different distances from target with 5 m diameter pool fire*

Correlation number	Correlation reference	Equation	Heat flux (kW m^{-2})		
			2 m	5 m	20 m
1	Mudan method	Equation 32	22	13	3
2	Shokri and Beyler	Equation 33	18	8	1
3	Point source model	Equation 34	20	16	4

6. Pool fire simulation

The aim of **Chapter 0** is to find and suggest a TEA solution substitute for testing fire protection systems experimentally at the industrial level. Fire Dynamic Simulation (FDS) was done on various hydrocarbon compounds to check which one behaved the most like TEA solution regarding the flame geometry. There is a lack of information and experiments with TEA solutions due to their high reactivity, pyrophoricity, and complex handling. Therefore, finding a less hazardous substitute that can be managed more easily may simplify conducting further tests and analyses for TEA solutions.

6.1 Introduction to FDS

To simulate fire behavior, Computational Fluid Dynamics (CFD) models numerically solve partial differential equations that explain mass, momentum, and energy conservation in fluid flow. Sub-models must also be included because of fires' chemical and physical processes. The empirical model and the CFD model are the two most popular forms of fire models. Fire engineers usually employ empirical fire models, which are popular due to their ability to generate highly accurate estimations of general fire conditions quickly. However, fire modeling is currently undergoing a phase of development, and with increased computational capacity, CFD models are becoming a more viable alternative for use in fire engineering. The Fire Dynamic Simulation (FDS) is at the cutting edge of new fire model advances. The FDS is a CFD model that uses a type of partial differential equations pool fire modeling suitable for low-speed, thermally-driven flow, focusing on smoke and heat transmission from fires (McGrattan & Forney, 2004).

The main sub-model of the FDS is the hydrodynamic model, which solves partial differential equations representing mass transport, momentum, and energy. These equations describe the low-speed movement of gases caused by chemical heat release and buoyant forces, which allows for wide variations in density, temperature, and small pressure changes. The equations are calculated in FDS using the simulation approach Large Eddy Simulation (LES) or Direct Numerical Simulation (DNS), which is dependent on the user needs or mesh resolution. In computing fluid dynamics, LES is a mathematical model for turbulence, and DES is a numerical model for solving the equations without any turbulence (McGrattan & Forney, 2004).

Another major sub-model in FDS is the combustion model. Depending on the size of the computational domain, the combustion process can also be modeled using the LES or DNS approaches. The DNS approach can model combustion if the computing domain is small enough. The diffusion of oxygen and fuel during combustion can be directly represented with DNS; however, because a highly dense mesh is required, this can only be done for tiny fires and in a small domain around a fire. If the mesh is not

fine enough, LES is a good option. LES is an FDS default unless the user specifies otherwise (McGrattan & Forney, 2004).

There are two techniques to model combustion. The reaction of fuel and oxygen is infinitely fast by default and is only controlled by mixing; alternatively, the reaction could be finite-rate. Most FDS applications involve a single step, a chemical reaction controlled by mixing. Accordingly, the reaction rate is infinite and only limited by the concentration of species that contains three lumped species as air, fuel, and products. The combustion model considers a single fuel species made up mostly of C, H, O, and N that interacts with oxygen in a single mixing-controlled phase to produce H_2O, CO_2, soot, and CO (McGrattan & Forney, 2004).

The key essential input data will be detailed in the following sections in order to replicate the desired scenario and receive the desired parameters in the output.

6.1.1. FDS inputs

The input file contains information about the geometrical configuration (the computational domain, geometrical structures, and mesh size), material properties and atmospheric conditions for the fire scenario.

6.1.1.1. The geometrical configuration

In the FDS, geometrical structures are confined within a computational domain, where the size and position of the coordinate system must be defined. The outer bounds of the computational domain are considered solid boundaries maintained at ambient temperature unless otherwise specified; the same is true for any structures added to the domain. The computational domain may consist of one or more rectangular meshes, each of which is divided into rectangular cells of varying sizes. The number of cells used will have a significant impact on the outcomes. A finer mesh with more cells is preferable, but it requires more computer resources (huge Random Access Memory (RAM) and run-time) and is thus more expensive, whereas a mesh with too many cells produces big mistakes. The structure is inputted as a set of rectangular obstructions since all geometric structures in the domain must conform to this rectangle mesh. The user determines the size of the computational domain and the number of mesh cells (McGrattan & Forney, 2004).

6.1.1.2. The material properties

The FDS requires several material properties as input, most of which are connected to the fuel or solid structures. The fuel can be a solid, liquid, or gas. The substances' properties consist of density, specific heat, thermal conductivity, the heat of combustion, heat release rate per unit area, the fraction of the

fuel amount converted to soot and carbon monoxide, and the fraction of heat radiated. The FDS requires information regarding density, thermal conductivity, specific heat, and emissivity for solid structures. Because values for individual materials may not be readily available depending on the application, the FDS literature includes a database of thermal properties for common materials (McGrattan & Forney, 2004).

6.1.1.3. Atmospheric conditions

The FDS input file must include the atmospheric condition inputs, such as wind speed, relative humidity, and ambient temperature; otherwise, the FDS will use default values. The default setting for relative humidity is 40%. The default temperature is 20 (ºC), whereas the ambient temperature is the temperature of everything at the start of the simulation. The wind speed can be constant or changeable depending on the height of the domain (McGrattan & Forney, 2004).

6.1.2. FDS output

At each time step, the FDS calculates radiant heat flux, temperature, density, pressure, velocity, chemical composition, and other variables within each numerical mesh cell. Prior to the start of the simulation, the intended output data must be defined in the input file. The output is usually in the form of enormous data files, which can be viewed in a graphical application called Smoke view (McGrattan & Forney, 2004).

As part of a fire dynamic simulation, the Smoke view is an external visualization tool that displays the results of the simulation. The Smoke view uses quantitative and realistic techniques to show smoke and other fire properties. To display smoke view, quantitative techniques such as 2D and 3D contouring are used. Realistic data display aims to show data the same way it would appear in real life (Forney, 2013).

6.2. FDS Case studies

In this case study, a liquid pool with a defined burning rate ($kg \cdot m^{-2} \cdot s^{-1}$) from **Table 31** burns in a 4 m by 5 m steel square tray with a 30 cm thick fuel layer shown in black. Steel properties were defined based on **Table 30.**

***Table 30**. Material properties of **steel** (McGrattan, 2006).*

Material	Emissivity	Density (kg m^{-3})	Conductivity	C_p
Steel	1	7850	45.8	0.46

The pool fire surface is defined in yellow. **Figure 11** illustrates the domain's representation, which has a 10 m by 10 m size with a 30 m height. The simulation was performed for 100 s fire duration, enough for the fire to reach the steady-state condition, with a cell size of 30 cm. In general, as the cell size gets smaller, the simulation results get more precise, but the time required increases. The simulation was run in various cell sizes of 10, 20, 30, and 40 cm. As a result, the 30 cm cell size was chosen as the optimum option in terms of accuracy and time required.

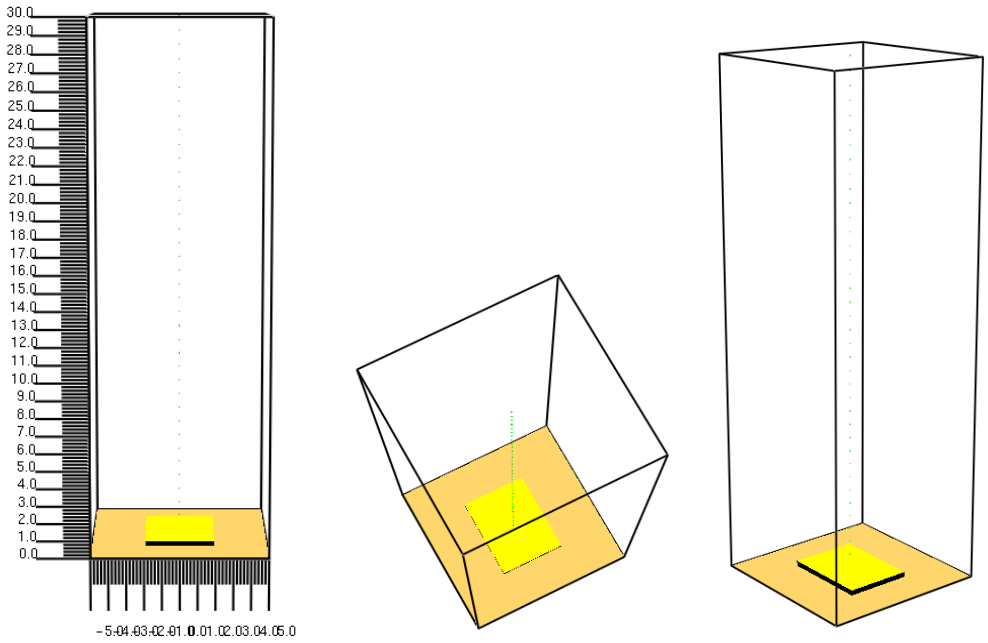

***Figure 11.** Pool fire case study domain.*

FDS has been performed for all the substances in **Table 31** in order to find a substance which can have close flame behavior to TEA solution. Hydrocarbon substances like n-hexane, n-octane, and benzene were chosen to have sufficient and close quantities of combustion and vaporization heat to TEA. The thermal properties of the substances, are presented in **Table 31**. FDS version of **6.7.7** has been used in this thesis (McGrattan & Forney, 2004).

Table 31. *Thermal properties of hydrocarbon chemicals and TEA solution.*

Product	ΔHc (kJ kg^{-1})	ΔHv (J g^{-1})	$\dot{m}''$ (Kg m^{-2} s^{-1})
TEA	-44694	536	0.053
11%TEA/Isopentane	-48110	363	0.087
N-Hexane	-37600	335	0.084
Benzene	-41831	383	0.086
N-Octane	-44420	301	0.083

Calculating the average flame height was the first goal of this chapter to find the best substitution for TEA and its solution. There were two ways of measuring average flame height with FDS output. After achieving a steady-state behavior of the flame at the end of the simulation, the simplest method was to use the ruler. A more accurate way was to plot the accumulated heat release rate per unit length (Acc. HRRPUL) versus height. A steady line should be reached which shows the independency of energy to height. At this point, 95% to 99% of total accumulated HRRPUL was calculated. Then, this value was placed in-between the table of the accumulated HRRPUL in excel, and the correspondent average flame length was selected. The explained procedure for finding the average flame height can be clarified and understood better in the following sections with the demonstrated figures and tables.

6.2.1. TEA case study

The case study domain, obstruction geometry, and property were determined in the section before. Then it is necessary to specify the fuel reaction and its characteristics. Since TEA is not a predefined chemical in FDS, the combustion reaction of TEA needed to be defined as **Equation 35** (Gonçalves et al., 2018).

$$C_6H_{15}Al + 6.25\,O_2 + 6.25(3.76\,N_2) \rightarrow AlO_2 + 7.5\,H_2O + CO + 4C + CO_2 + 23.51\,N_2 \quad \textit{Equation 35}$$

After specifying the combustion elements and their volume fractions from the reaction, the heat of combustion of TEA was used as -44694 ($kJ \cdot kg^{-1}$). Clarifying the fuel characteristics can be done with many different parameters which was explained before in the material section. Here, it has been decided to use the computed mass flux of TEA as 0.053 ($kg \cdot m^{-2} \cdot s^{-1}$) to define the fuel property.

The last step before running the simulation was setting different sensors through the fire to extract the required output in order to obtain the average flame height, temperature, and heat release rate.

Figure 12 illustrates the flame behavior of the TEA at the second of 100. The heat release rate of the solution was stabilized and reached the maximum of 48 MW in 100 seconds. The flame size of 9 m was estimated from **Figure 12** with the marked ruler.

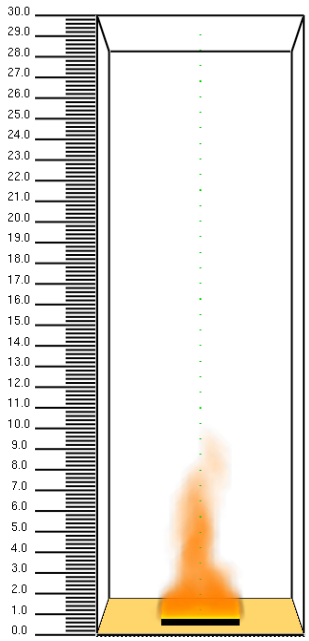

Figure 12. *FDS simulation for **TEA** pool fire with 5 diameters (flame was predicted 9 m) at 100 s.*

The Heat Release Rate Per Unit Length (HRRPUL) versus height was plotted from output data in **Figure 13**. The sharp increase was initially attributed to the discharge of significant energy in comparison to the flame height, but as the height was increased, the abrupt spike began to fade. HRRPUL obtains a value of zero after approximately 9 m from the surface, showing that the energy with height is no longer increasing and the fire has reached a stable state.

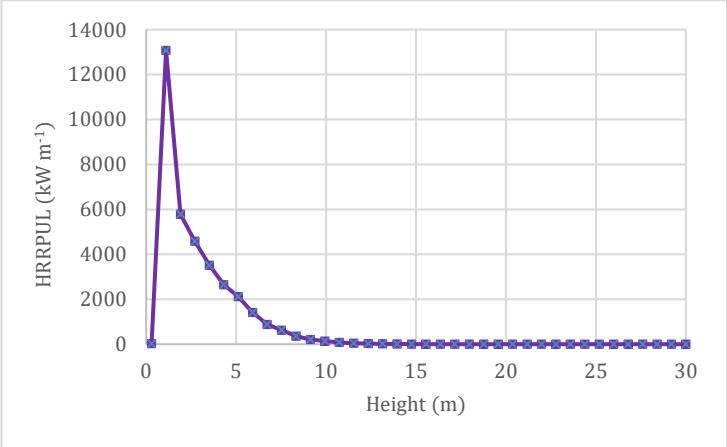

***Figure 13. TEA** HRRPUL versus height.*

Plotting the accumulated heat release rate per unit length (Acc. HRRPUL) versus the height illustrated in **Figure 14** was the preferable method for estimating the more accurate average flame height. The 95% to 99% of total accumulated HRRPUL (35566 kW·m^{-1}) was calculated as 35210 (kW·m^{-1}). Therefore, a value of 35210 (kW·m^{-1}) was placed between the accumulated HRRPUL table in output data, a part of which is shown in **Table 32**. The accumulated HRRPUL of 35210 (kW·m^{-1}) was found between the colored cells, which corresponds to the average flame length of around 9 meters.

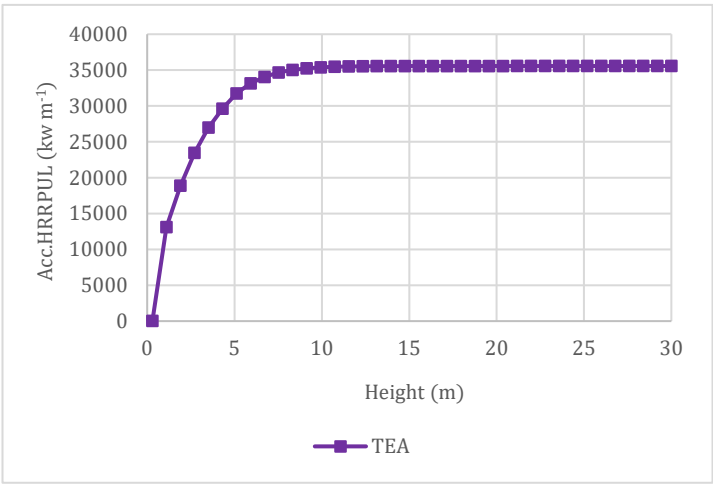

***Figure 14**. **TEA** accumulated HRRPUL versus height.*

***Table 32. TEA** accumulated HRRPUL versus height.*

Neat TEA	
Height (m)	**Acc. HRRPUL (kW m^{-1})**
7	34663
8	35027
9	35235
10	35377

The temperature profile in different regions is another significant factor in the fire simulation. From bottom to top, a fire flame consists of three main parts: continuous flame, which indicates the physical existence of flame continually; intermittent flame, which may be observed as on and off; and the final part is a buoyant plume with no physical evidence of fire but still hot gases. Hot gases in the plume can be detected using sensors and smoke detectors. The plume temperature is essential to be analyzed to determine where the extinguisher should be placed on top of the expected pool fire so that it can melt and be functionalized. Although a flame height of 9 meters was obtained for the TEA pool fire, **Figure 15** proves the existence of hot gases with a high temperature of 351 (ºC) still to a distance of 24 meters above the surface.

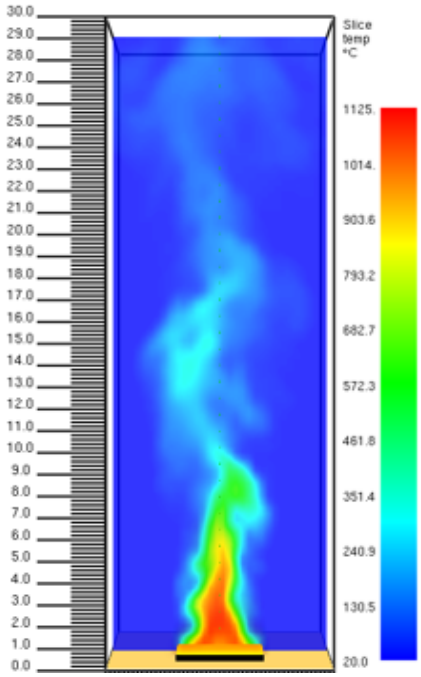

***Figure 15.** Temperature profile of **TEA** pool fire with 5 diameters.*

6.2.2. TEA solution case study

In industry, TEA solution is preferred over TEA because of its lower reactivity, lower cost, greater availability, and ease of use. Different types of solvents like n-hexane, isopentane, diethyl ether or tetrahydrofuran. TEA solution in isopentane has picked this thesis attention because of its extreme fire behavior and capacity to achieve a higher burning rate (0.087 $kg \cdot m^{-2} \cdot s^{-1}$) compared to other solutions.

The same process has been applied to the simulation of 11%TEA/isopentane. It has been assumed that the fuel combustion reaction will be expressed in terms of heat of combustion of -48110 ($kJ \cdot kg^{-1}$). Additionally, TEA solution characteristics have been defined based on 0.087 ($kg \cdot m^{-2} \cdot s^{-1}$) mass flux, which was calculated in the previous chapter.

Figure 16 shows the flame behavior of the TEA solution after 100 seconds. In 100 seconds, the heat release rate of the solution reached a maximum of 82 MW. **Figure 16** was used to estimate the flame size of 13 m using the designated ruler.

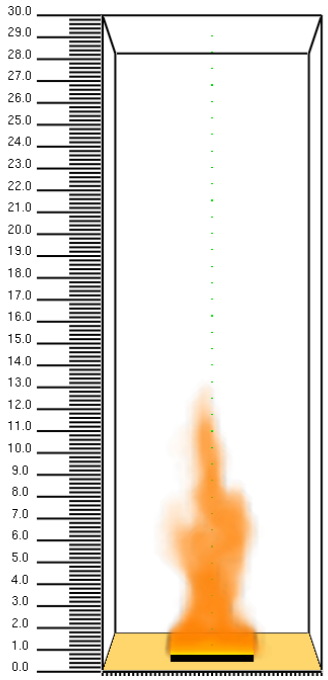

***Figure 16**. FDS simulation for **TEA solution** pool fire with 5 diameters (flame was predicted 13 m) at 100 s.*

Figure 17 shows how the rate of releasing energy has been changing with height. The same trend as TEA in **Figure 13** has been achieved, with the exception that the zero amount was reached at a greater height. The steady-state was achieved at the point of 13 m.

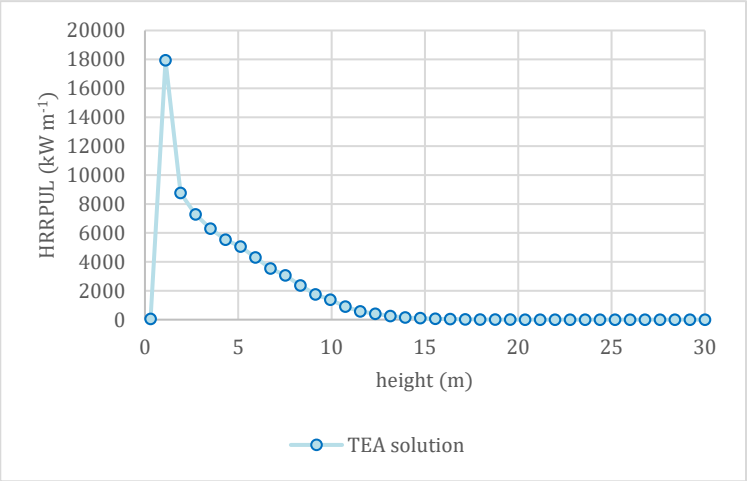

***Figure 17. TEA solution** HRRPUL versus height*

Figure 18 shows the recommended method of plotting the accumulated heat release rate per unit length (Acc. HRRPUL) versus height. 69300 ($kW \cdot m^{-1}$) was computed as the 95% to 99% of total accumulated HRRPUL (70000 $kW \cdot m^{-1}$). Accordingly, a value of 69300 ($kW \cdot m^{-1}$) is equal to a flame length of 13 meters on average in **Table 33**.

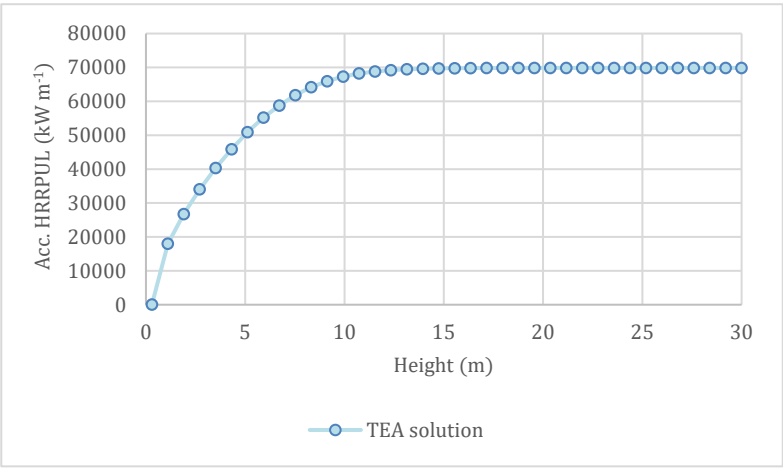

***Figure 18. TEA solution** accumulated HRRPUL versus height.*

***Table 33. TEA solution** accumulated HRRPUL versus height.*

TEA solution	
Height (m)	**Acc. HRRPUL (kW m^{-1})**
11	68791
12	69203
13	69390
14	69603

Despite the fact that the TEA solution pool fire reached a flame height of 13 meters, **Figure 19** shows the presence of hot gases with a temperature of 351 degrees Celsius till a distance of 27 meters above the surface.

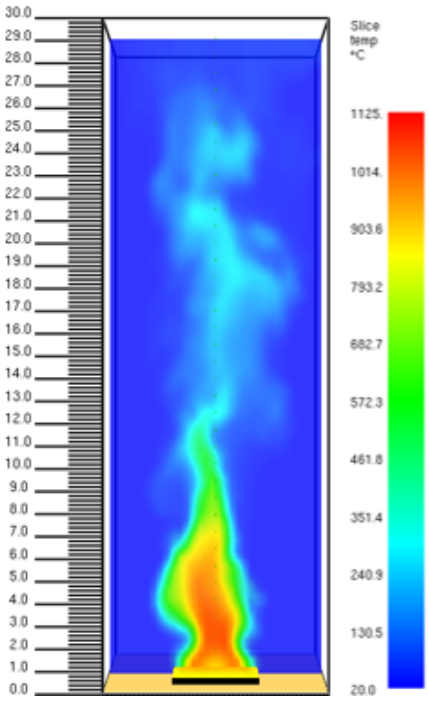

***Figure 19**. Temperature profile of **TEA solution** pool fire with 5 diameters.*

6.2.3. N-Hexane case study

Hexane is an organic material with the chemical formula C_6H_{14}. It is a straight-chain alkane containing six carbon atoms, and it is a transparent liquid with no odor or color. It can be used as a non-polar solvent that is relatively safe, mainly unreactive, inexpensive, and quickly evaporated. Hexane can be found in manufacturing glues for shoes, roofing, and leather goods. They can also extract frying oils from seeds (such as soy or canola oil), sanitize and clean various stuff, and manufacture fabrics (McKee et al., 2015).

Hexane has lower toxicity and reactivity than TEA, making it a good substitute for studies. However, the National Fire Protection Association (NFPA) has assigned n-hexane a flammability code of 3 (slight) and a health hazard identification code of 1 (serious). Prolonged exposure to n-hexane or a concentration higher than 5000 ppm can pose a health risk (NFPA, 1994).

The same procedure as TEA was used to simulate n-hexane pool fire. Because n-hexane is a predefined substance in FDS, there is no need to define its reaction. For the combustion process, a heat of combustion of -37600 ($kJ \cdot kg^{-1}$) was introduced. The n-hexane burning rate should have been computed in order to characterize the compound properties. Thermochemistry data from **Table 34** was employed in the Mudan equation, yielding a maximum mass flux of 0.84 ($kg \cdot m^{-2} \cdot s^{-1}$) for n-hexane.

***Table 34**. **N-Hexane** condensed phase thermochemistry data* (NIST, 2022a).

Substance	Cp kJ (kg^{-1} K^{-1})	T_b (ºC)	ΔHc (kJ kg^{-1})	ΔHv (J g^{-1})	$\dot{m}''$ (kg m^{-2} s^{-1})
N-Hexane	2.27	68.7	-37600	335	0.084

In order to obtain the n-hexane flame length, the same steps have been repeated in **Figure 20** and **Figure 22**. The fire simulation of n-hexane is shown in **Figure 20**, which estimates the flame height of 14 m. In this case, 67 MW was determined to be the maximum heat release rate after 100 seconds.

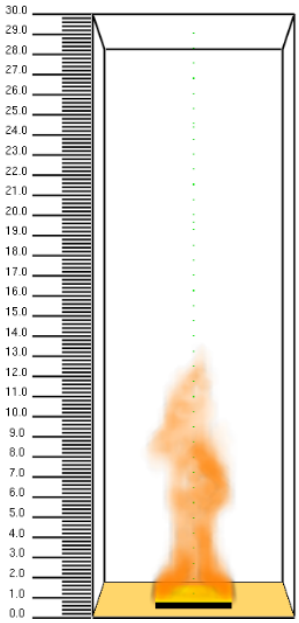

***Figure 20**. FDS simulation for **N-Hexane** pool fire with 5 diameters (flame was predicted 14m).*

In comparison to TEA and its solution, a smoother trend in heat release rate reduction was found. Although the maximum energy produced by the fuel was smaller than that released by TEA and its solution, it required longer to attain a steady state. As a result, at a height of roughly 15 meters, the value of zero was obtained in **Figure 21**.

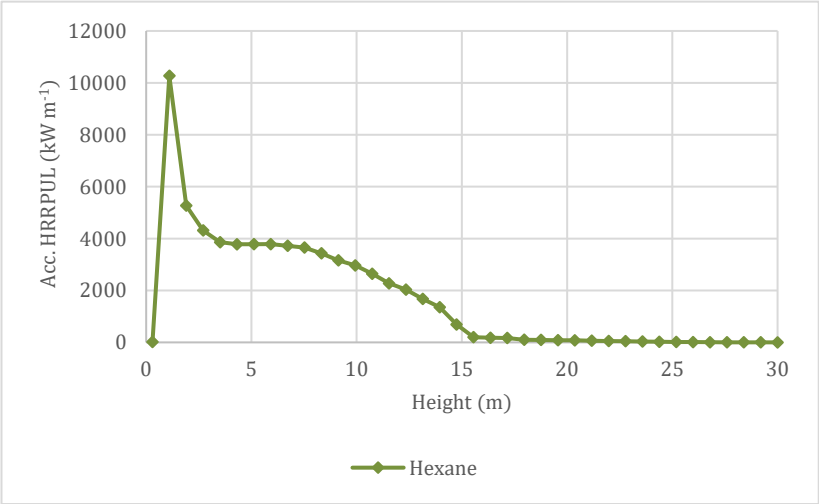

***Figure 21. N-Hexane** HRRPUL versus height.*

Figure 22 demonstrate the effect of height on heat release rate at various points. The 95% to 99% of total accumulated HRRPUL (65571 kW·m^{-1}) was computed 62293 (kW·m^{-1}), and the result of approximately 14 m average flame height has been selected as the best match with 62293 (kW·m^{-1}) in **Table 35**.

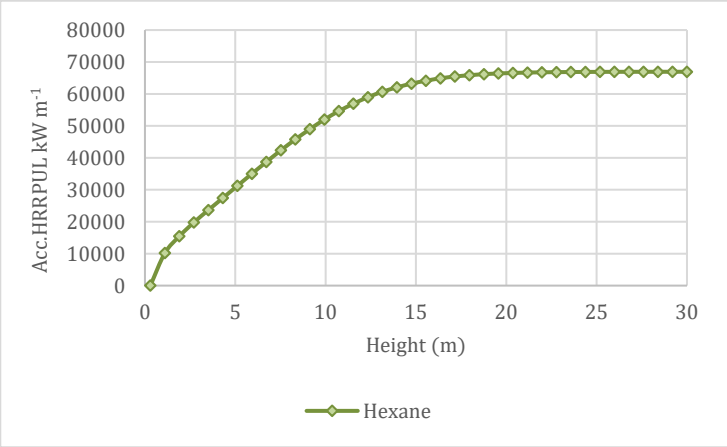

***Figure 22**. **N-Hexane** accumulated HRRPUL versus height.*

***Table 35. N-Hexane** accumulated HRRPUL versus height.*

N-Hexane	
Height (m)	**Acc. HRRPUL (kW m^{-1})**
13	60643
14	62000
15	63185
16	64924

The temperature distribution of an n-hexane pool fire is visualized in **Figure 23**. As was expected, the high range temperature of 351 to 462 (ºC) has been observed for the plume area to help fire engineers be alert to potential hazards in the distance at least 27 meters above the pool fire surface.

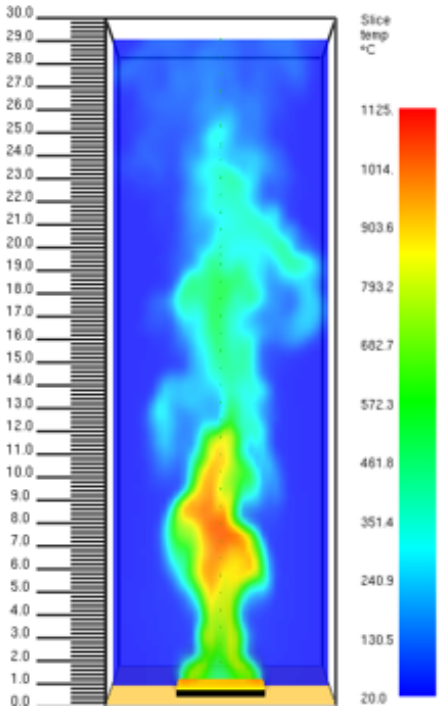

Figure 23. *The temperature profile of the* ***N-Hexane*** *pool fire with 5 diameters.*

6.2.4. N-Octane case study

N-octane is an eight-carbon-atom straight-chain alkane with the formula $C_8 H_{18}$. It is a colorless liquid with a gasoline odor. Water-insoluble and less dense than water. Therefore, it floats on water and emits a strong odor. N-Octane is a flammable liquid that can be lethal if swallowed and inhaled for a long time(NIH, 2022). N-Octane may be incompatible with potent oxidizing agents and pyrophoric substances like TEA. Burning may occur, followed by igniting unreacted material and other nearby combustibles, and not affected by aqueous solutions of acids, alkalis, most oxidizing agents, and most reducing agents. When heated sufficiently or ignited in the presence of air, oxygen, or potent oxidizing agents, it burns exothermically to produce primarily carbon dioxide and water (ROTH, 2015). **Table 36** has been used in order to simulate the n-octane pool fire.

***Table 36**. **N-Octane** condensed phase thermochemistry data* (NIST, 2022c)

Substance	Cp kJ (kg^{-1} K^{-1})	T_b (ºC)	ΔHc (kJ kg^{-1})	ΔHv (J g^{-1})	$\dot{m}''$ (kg m^{-2} s^{-1})
N-Octane	2.23	125.6	-44420	301	0.083

Figure 24 shows the flame behavior of n-octane after 100 seconds. The heat release rate of n-octane was obtained as 73 MW at the corresponded time. The defined steps explained about TEA have been performed for n-octane and can be seen in **Figure 24** and **Figure 26**.

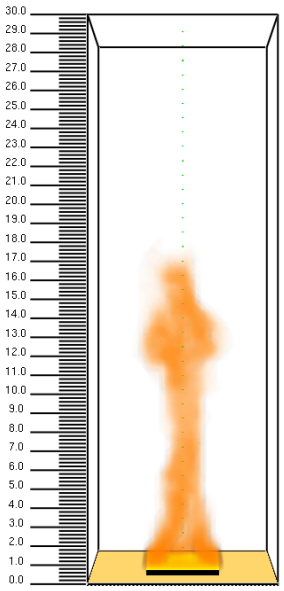

***Figure 24**. FDS simulation for **N-Octane** pool fire with 5 diameters (flame was predicted 17m).*

Same trend as n-hexane was achieved for n-octane in **Figure 25**. Getting stabilized approximately at the distance of 20 m from the surface.

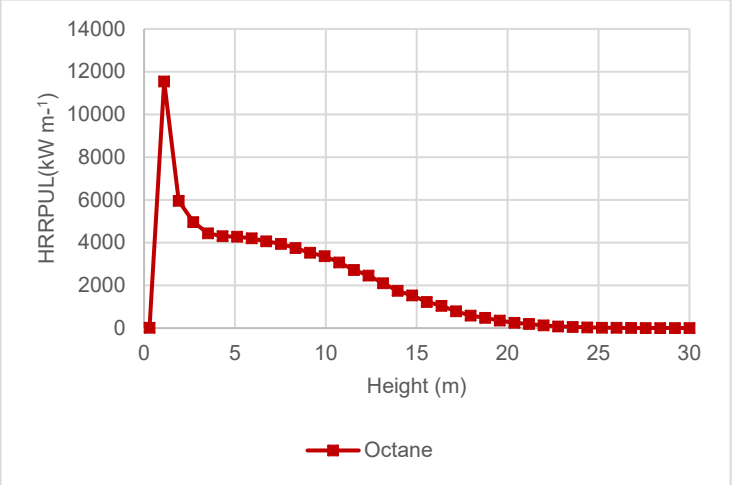

***Figure 25. N-Octane** HRRPUL versus height.*

In **Figure 26**, the 95% to 99% of the total accumulated HRRPUL (77228 kW·m^{-1}) was calculated as 73366 (kW·m^{-1}). The average flame length of 17 m was found to be the equivalent result when this value was fitted in-between the **Table 37**.

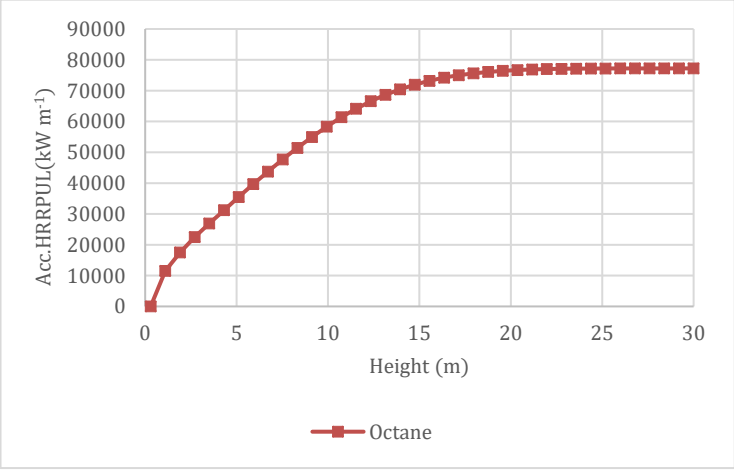

***Figure 26. N-Octane** accumulated HRRPUL versus height*

Table 37.N-Octane *accumulated HRRPUL versus height*

N-Octane	
Height (m)	**Acc. HRRPUL (kW m^{-1})**
15	71956
16	73181
17	74225
18	75012

According to the n-octane temperature profile, shown in **Figure 27**, high temperatures range from 452 to 793(ºC) until a distance of 23 meters above the surface and 241 to 351(ºC) till 28 m were observed. As a result, high temperatures pose a threat at least 30 meters over a pool fire's level.

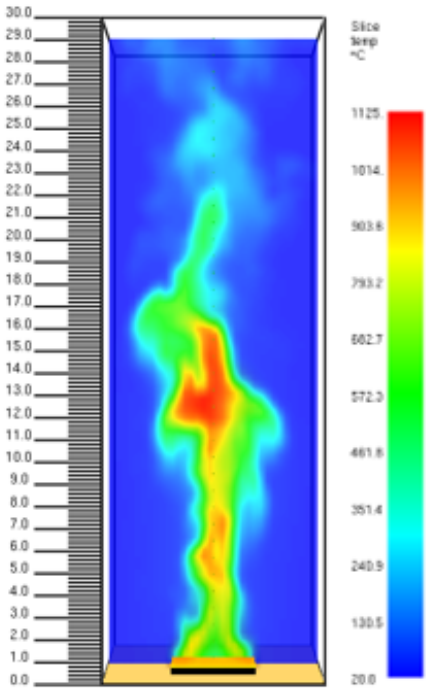

Figure 27*. The temperature profile of the* ***N-Octane*** *pool fire with a diameter of 5 m.*

6.2.5. Benzene case study

Benzene is a colorless or light-yellow liquid at room temperature with the formula of C_6H_6. It is highly combustible and has a sweet odor. Benzene evaporates fast into the atmosphere. Because its vapor is heavier than air, it may settle in low-lying places. Benzene just slightly dissolves in water and floats on top of it. Benzene is utilized in the manufacturing of polymers, resins, nylon, and synthetic fibers in several sectors. Benzene is also used to create lubricants, rubbers, dyes, detergents, medicines, and pesticides, among other things (NCEH, 2018).

People who breathe in very high doses of benzene may experience the following symptoms within minutes to several hours: Dizziness, headaches, confusion, unconsciousness and death. Direct benzene exposure to the eyes, skin, or lungs can cause tissue damage and discomfort (NCEH, 2018). Compared to n-hexane and n-octane is more risky and harder to be handled. So, it can't be the best option but still is less risky than TEA in terms of self-ignition.

Benzene is also a predefined compound in FDS. Data presented in **Table 38** has been used to define the combustion reaction and property of benzene with heat of combustion of -41831 ($kJ \cdot kg^{-1}$) and burning rate of 0.086 ($kg \cdot m^{-2} \cdot s^{-1}$).

Table 38. Benzene *condensed phase thermochemistry data* (NIST, 2022a).

Substance	Cp **kJ (kg^{-1} K^{-1})**	T_b **(ºC)**	ΔHc **(kJ kg^{-1})**	ΔHv **(J g^{-1})**	$\dot{m}''$ **(kg m^{-2} s^{-1})**
Benzene	1.72	80	-41831	383	**0.086**

Figure 28 depicts the benzene's flame behavior at the second of 100. The heat release rate was stabilized, reaching a maximum of 71 MW in 100 seconds. With the designated ruler, the flame size of 16 m was determined from **Figure 28**.

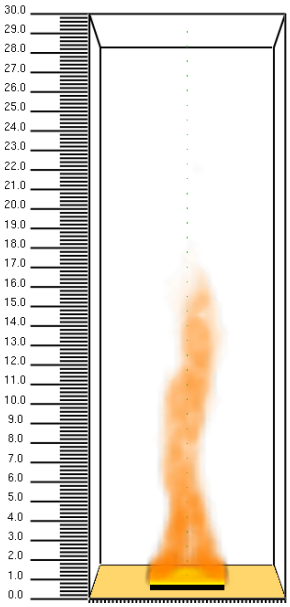

***Figure 28**. FDS simulation for **Benzene** fire with 5 diameters (flame was predicted 16 m) at 100 s.*

Before using the second method, it was better to plot the benzene HRRPUL versus the distance horizontally from the surface of pool fire to make sure the steady behavior of benzene flame has been achieved during the first 100 seconds.

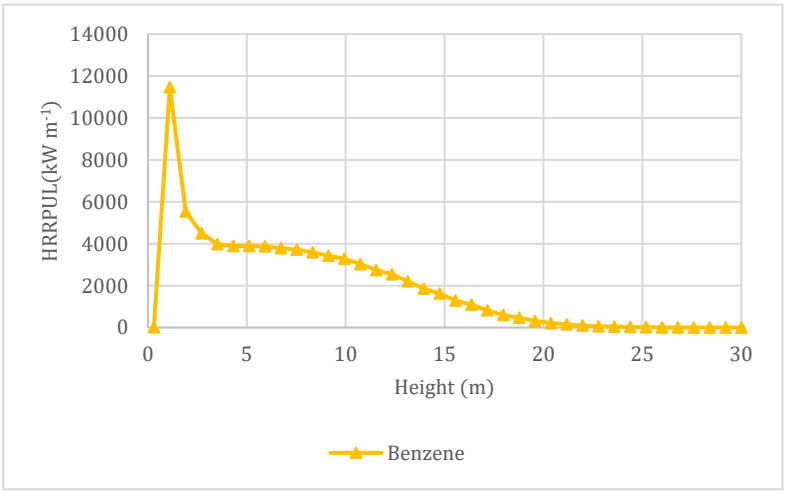

***Figure 29. Benzene** HRRPUL versus height.*

In the same way as the other four chemicals, in **Figure 30** 95% to 99% of the total accumulated HRRPUL (74213 kW·m^{-1}) was computed as 70503 (kW·m^{-1}). Then, the obtained amount was placed in-between the out table of the accumulated HRRPUL that a part is shown in **Table 39**, and it was observed that the average flame length of 16 m was the correspondent one. The achieved behavior was so close to n-octane flame.

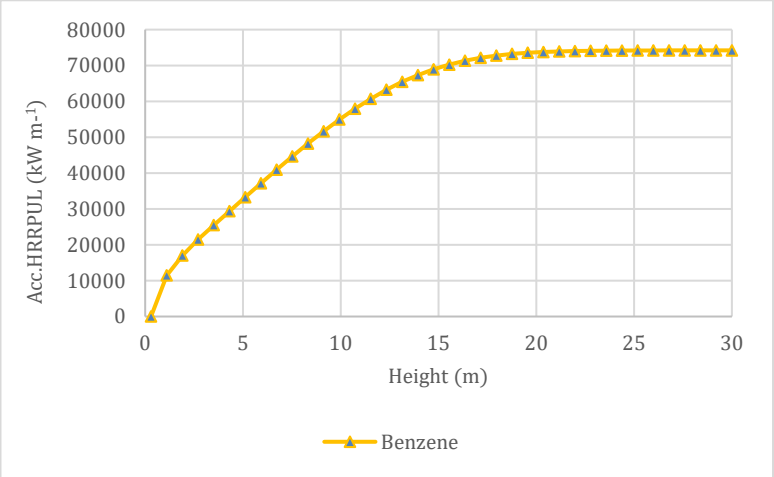

***Figure 30. Benzene** accumulated HRRPUL versus height.*

***Table 39. Benzene** accumulated HRRPUL versus height.*

Benzene	
Height (m)	**Acc. HRRPUL (kW m^{-1})**
14	68949
15	70245
16	71337
17	72161

Based on the temperature profile of benzene in **Figure 31**, high temperatures extend from 351 to 733 (ºC) to a distance of 26 meters and 240 to 351 (ºC) to 30 m far from the surface. As a result, high temperatures threaten at least 32 meters above a pool fire's surface. Despite the fact that n-octane has a higher flame height, the benzene temperature profile shows a higher temperature for the plume area, which can be affected by a variety of factors, including chemical composition, rate of fuel combustion, pressure, density, and thermal conductivity of the substance.

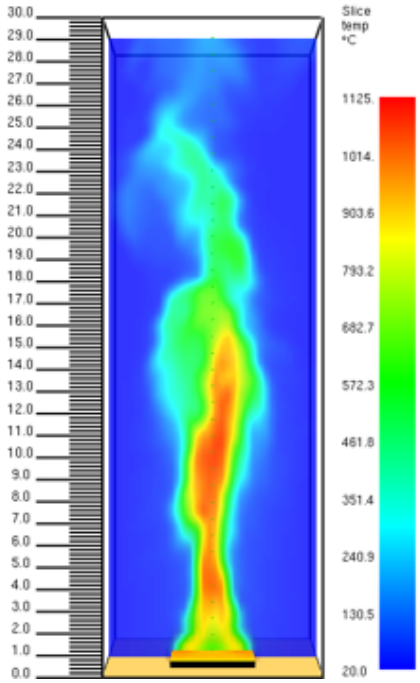

Figure 31. *The temperature profile of the* ***Benzene*** *pool fire with a diameter of 5 m.*

6.2.6. Comparison and results

Various flame heights and behaviors were detected after simulating the target chemicals and presented in **Table 40**. Plotting the accumulated heat release rate per unit length (Acc. HRRPUL) versus height, as illustrated in **Figure 32**, was a more accurate method.

Based on **Table 40**, the average flame heights simulated with FDS for neat TEA and 11%TEA/Isopentane match the values calculated in **Chapter 5**.

According to **Table 40**, n-hexane average flame height of 14 meters is the best option for future trials instead of the TEA solution and TEA with the flame height of 13 m and 9 m. **Figure 32** illustrates that the green line, which corresponds to n-hexane, has the closest behavior to the light blue line (TEA

solution) in flame height. N-octane, compared to others, reaches the steady behavior at a higher height (16 m).

Compared to other substances, the sharp increase of the TEA solution line in **Figure 32** is because of its high rate of releasing heat and energy in a short time which can also be justified with its high burning rate (0.87 $kg \cdot m^{-2} \cdot s^{-1}$) and heat of combustion (-48110 $kJ \cdot kg^{-1}$).The TEA solution's highest heat generating rate (82 MW) is significantly higher than TEA (48 MW). Experimental evidence and theoretical modeling predicted that TEA solution will behave worse than neat TEA due to its greater burning rate. In general, a solvent is added to a substance to make it easier to handle. Although the TEA solution behaves worse in an accident, it is more manageable and easier to be handled in terms of reactivity. The pyrophoricity of pure TEA is higher than TEA solution, allowing it to ignite without an ignition source and is so risky. Another factor is the type of solvent; among all the solutions in **Chapter 4**, the burning rate of 11%TEA/isopentane was the highest and had the worst flame behavior. The simulation results also confirmed that adding solvent to pure TEA can affect both the thermal and geometric behavior of its fire.

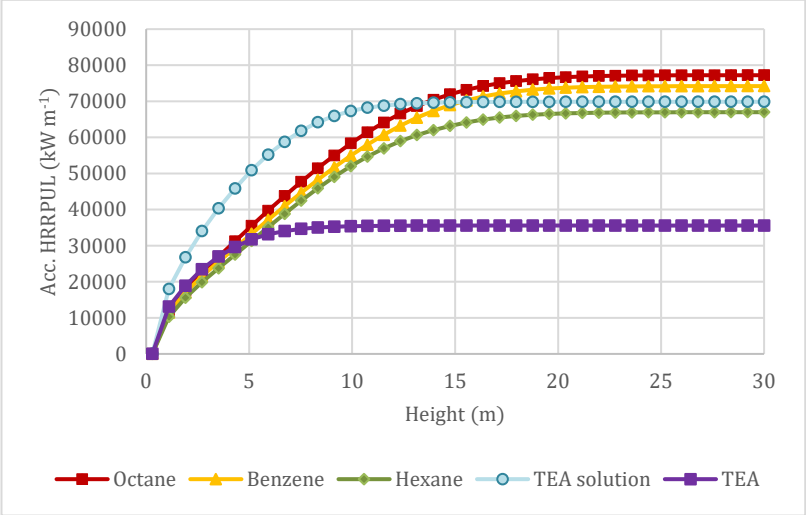

***Figure 32**. Chemicals accumulated HRRPUL versus height.*

***Table 40.** Results comparison of flame height and heat release rate for chemicals.*

Substances	Average flame height (m)	Max HRR (MW)
TEA	9	48
TEA solution	13	82
N-Hexane	14	67
Benzene	16	71
N-Octane	17	73

6.3. Advantages and drawbacks of different approaches

Different approaches have been done in previous sections for both neat TEA and TEA solution. In all methods the flame height of the TEA solution was around 13 m. Theoretical modeling varied slightly in several correlations, but the best recommended correlation, the Thomas equation, yielded a flame height of 13 meters.

Generally, the results from different approaches are not as good as those obtained for the TEA solution, and they are different. The pros and cons of each methodology for determining the flame height are presented and compared in **Table 41** based on the TEA results and data.

***Table 41**. Advantages and disadvantages of different methodologies for determining the flame height.*

Approaches	TEA flame height	Advantage	Disadvantage
Experiment	7 m	1. Accurate	1. Risky and hard to handle
		2. Fast	2.Expensive
			3.Hard to change the conditions
Theoretical	10 m	1. Safe	1. Less precise
		2. Mostly accurate	2. Vary with different correlations
		3. Easy to change conditions	3. Slow
		4. Cheap	4. Human error
Simulation (FDS)	9 m	1. Safe	1. Complex
		2. More accurate than theoretical modeling	2. Less accurate than experiment
		3. Easy to change conditions	3. Slow and time consuming
		4. Cheap	
		5. Less human error	

7. Study of a fire protection system for TEA storage

This chapter is aimed to studying the fire protection system for TEA storage after learning about the fire behavior of TEA in the event of a pool fire. Accordingly, the acceptable vertical distance from the fire should be measured in order to determine where an extinguisher should be placed in a typical fire prevention system configuration, as illustrated in **Figure 33**.

Figure 33 shows a top view of alkyl-aluminum storage like TEA. Four grey circled shapes at the bottom of the figure correspond to storage tanks which are supported with double-walled and made of steel to monitor the leakage. All the pipes should be supported with stainless steel holders to prevent corrosion. The storage tanks are usually situated on a concrete drainage surface. To reduce the heat load on the tanks in the event of a fire, any product leakage is routed through drain holes below the fire wall into a burn-trench behind the fire wall. A second fire wall is used to protect the burn trench. As it was marked in blue in **Figure 33**, the burn-trench is covered with plastic bags of suitable extinguishing agents (e.g., vermiculite powder and sand). Vermiculite-filled plastic sacks are often used in burning trenches and pits. Once the sacks melt, the material spreads across the surface, decreasing the oxygen supply (Heyn, 2015) and suppressing the fire.

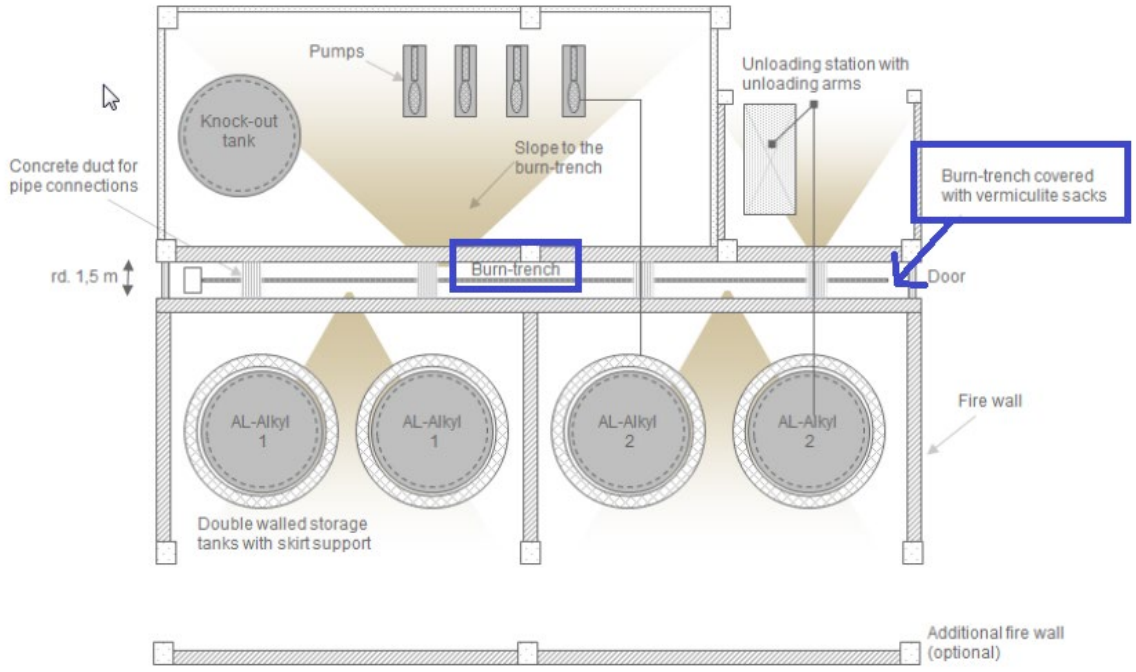

Figure 33. Top view *for the storage of aluminum alkyl solutions* (Heyn, 2015).

Following the estimation of the flame height and the selection of n-hexane for further research, it was determined to consider thermal radiation intensity ($kW \cdot m^{-2}$) and temperature (ºC) at various vertical distances from the pool surface as critical elements in extinguisher placement. Heat flux sensors were placed on the vertical axis with a minus-three orientation (negative side of Z axis). Heat flux and temperature sensors were used to track changes in heat flux as a function of height.

On an average of 10 minutes of exposure, **Table 42** demonstrates the different ranges of thermal intensity ($kW \cdot m^{-2}$) for industry equipment. The package containing vermiculite or sand extinguishers is made of plastic, and according to **Table 42**, a heat flux of 12.5-15 ($kW \cdot m^{-2}$) can cause melting. In the case of adequate packaging, a heat flux of 15 ($kW \cdot m^{-2}$) and above was established as an acceptable level.

***Table 42**. Industry equipment's vulnerability on an average **10 minutes** exposure time* (Gerald William Wellman, 2004).

Incident heat flux (kW m^{-2})	Type of damage
35-37.5	Damage to process equipment including steel tanks, chemical process equipment, or machinery
25	Minimum energy to ignite wood at indefinitely long exposure without a flame
18-20	Exposed plastic cable insulation degrades
12.5-15	Minimum energy to ignite wood without a flame; melts plastic tubing
5	Permissible level for emergency operations lasting several minutes with appropriate clothing

Various plastic packaging material and their melting temperature are given in **Table 43**. The highest melting point of 255 (ºC) corresponds to polyethylene terephthalate (PET). So, the minimum temperature of 255 (ºC) was considered an acceptable point to guarantee their melting phenomena.

***Table 43**. Density and melting point of different plastic types* (Karel Van Acker, 2018).

Plastic Type	Density (kg m^{-3})	T_m (◦C)
Polyethylene terephthalate (PET)	1350-1390	255
Polyvinyl chloride (PVC)	1100-1450	210
Polylactic acid (PLA)	1200-1450	155-165
Poly-3-hydroxybutyrate (PHB)	1300	180

As expected, temperature and heat flux showed the same trend in **Figure 34**. The reduction in temperature and heat flux as a function of height is also visible in this figure. According to **Table 42** and **Table 43** the heat flow must be greater than 15 ($kW \cdot m^{-2}$), and the temperature must be at least 255 (◦C) to activate the suppression system. So, 15 ($kW \cdot m^{-2}$) heat flow and a temperature of 258 (◦C) at 19 meters from the surface were determined as a threshold value. **Table 44** shows the extracted data for heat flux and temperature from the edge of flame (13 m) to the accepted point, highlighted in green. As a result, the vermiculate bags and burn trench in **Figure 33** should be designed between 13 and 23 meters above ground level.

Table 44. TEA solution fire *heat flux and temperature versus height.*

Height (m)	Heat flux ($kW\ m^{-2}$)	Temperature (◦c)
13	45	476
14	35	419
15	30	389
16	25	352
17	18	296
18	16	272
19	15	258
20	13	239

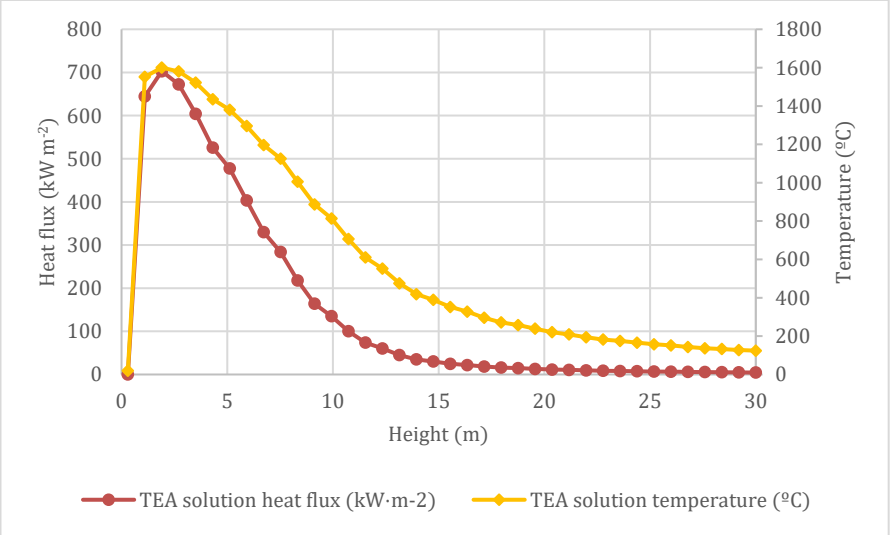

Figure 34. TEA solution *temperature and heat flux versus height.*

In the case of n-hexane, heat flux and temperature were within approved limits from the margin of flame (14 m) to the distance of 23 meters above the surface, following the heat flux of 15 ($kW.m^{-2}$) and temperature of 259 (°C) which are shown in **Figure 35**. Although the maximum temperature and heat flux received from n-hexane is much lower than the TEA solution, it will remain for more time and till a higher height above the flame. **Table 45** presents the output data corresponding to heat flux and temperature until the approved point, differentiated with green. So, the vermiculate bags and burn trench in **Figure 33** should be designed in the accepted range of 13 to 23 m above the ground.

Table 45. N-Hexane *heat flux and temperature versus height.*

Height (m)	Heat flux ($kW\ m^{-2}$)	Temperature (◦c)
13	127	664
14	106	603
15	92	562
16	74	507
17	51	433
18	41	395
19	35	373
20	29	345
21	20	301
22	17	279
23	15	259
24	13	247

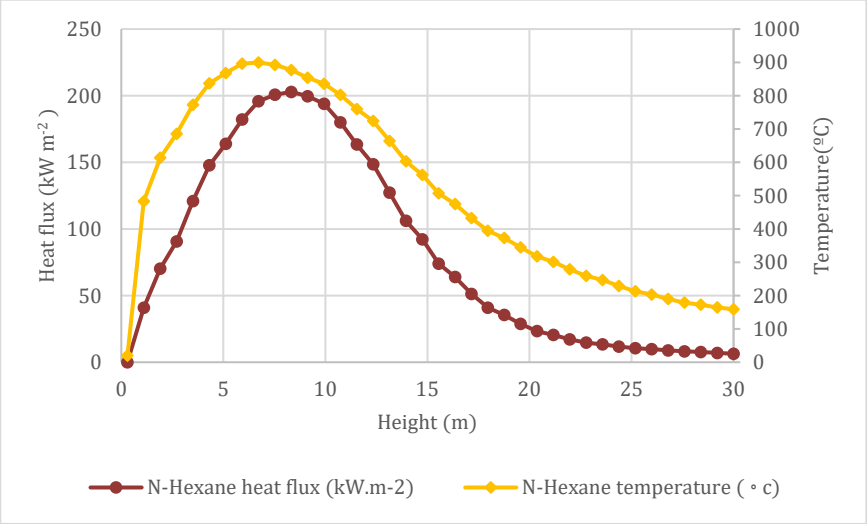

Figure 35. N-Hexane *temperature and heat flux versus height.*

8. Conclusions

In this thesis pyrophoric substances and their effects have been analyzed. Large-scale pool fires can be caused by the accidental release and leakage of pyrophoric liquid substances and can cause hazards due to radiant heat. Detailed knowledge of the radiant heat estimation methods was necessary to predict the likely hazards of these fires on adjacent facilities. Predicting the behavior of pool fire was analyzed with theoretical equations, experimental data, and simulations.

This thesis analyzes a large pool fire of 5 m diameter with a theoretical model and hand calculations. A flame height of 10 meters was achieved for neat TEA, resulting in a thermal radiation intensity which reduced from 18 to 1 $kW \cdot m^{-2}$ for horizontal distances of 2 to 20 meters. Calculations proved that adding solvent to pure TEA increases heat release and flame height. 11%TEA/isopentane resulted in the average flame height of 13 meters and heat flux of 20 to 4 $kW \cdot m^{-2}$ for horizontal distances of 2 to 20 meters far from the edge of fire. Heat radiation above 10 ($kW \cdot m^{-2}$) is life threatening and around 5 ($kW \cdot m^{-2}$)can still damage other facilities.

All the results calculated with theoretical models fit and were close to the experimental data. Although all the measurements were acceptable, there were inconsistencies between different methods because of various independencies in different correlations. Based on the results in **Chapter 5**, Burgess equation for burning rate, Thomas method for average flame height, Burgess and Hertzberg for emissive power and Shokri and Beyler and point source model for heat flux were selected as the best correlations.

After theoretical modeling of the TEA pool fire, FDS simulations have been performed on TEA, TEA solution fires and other hydrocarbons fires to suggest a safer potential substance to be used for experimental analysis of fire behavior. N-hexane, with a flame height of 14 meters and a maximum heat release rate of 67 MW, was the closest alternative to the TEA solution, with an average flame height of 13 meters and maximum heat release rate of 82 MW. N-Hexane is a safer substance to be used in terms of handling and reactivity for future fire tests. Further analysis has also been done on n-hexane and TEA solutions to indicate the appropriate height to place a fire protection system based on powder dispersion (e.g., vermiculite) from the top of the flames. Sensors in FDS were placed on the vertical axis above the flame to measure the temperature and heat flux for n-hexane and TEA solution fires. The heat flux above 15 ($kW \cdot m^{-2}$) and the minimum temperature of 255 (◦C) have been specified to ensure vermiculate bags' melting. This accepted range was achieved till 19 meters above the surface for TEA solutions and 23 meters for n-hexane.

9. References

AkzoNobel. (2008). *Metal alkyls and their solutions*.

AkzoNobel. (2010). *TEAL Product Data Sheet*.

Alnajjar, M. (2009). *Handling pyrophoric reagents*. http://www.ntis.gov/ordering.htm

Alnajjar, M., Quigley, D., Kuntamukkula, M., Simmons, F., Freshwater, D., & Bigger, S. (2011). Methods for the safe storage; handling; and disposal of pyrophoric liquids and solids in the laboratory. *Journal of Chemical Health and Safety*, *18*(1), 5–10. https://doi.org/10.1016/j.jchas.2010.03.001

Alymov, M. I., Seplyarskii, B. S., Vadchenko, S. G., Kochetkov, R. A., Rubtsov, N. M., Abzalov, N. I., & Ankudinov, A. B. (2020). Interaction of compact samples made of pyrophoric iron nanopowders with air. *Mendeleev Communications*, *30*(3), 380–382. https://doi.org/10.1016/j.mencom.2020.05.040

Anderson. (1963). *Asymptotic theory for principal component analysis*.

Aven, T. (2016). Risk assessment and risk management: Review of recent advances on their foundation. *European Journal of Operational Research*, *253*(1), 1–13. https://doi.org/10.1016/J.EJOR.2015.12.023

Bubbico, R., Dusserre, G., & Mazzarotta, B. (2016). Calculation of the flame size from burning liquid pools. *Chemical Engineering Transactions*, *53*, 67–72. https://doi.org/10.3303/CET1653012

Casal. (2017). *Evaluation of the effects and consequences of major accidents in industrial plants*.

Cotton & Wilkinson. (1972). Advanced-inorganic-chemistry. *Advanced-Inorganic-Chemistry*.

Forney, G. P. (2013). *Smokeview (Version 6)*. https://doi.org/10.6028/NIST.SP.1017-2

Gao, J., Man, X., Shen, J., Meng, Q., & Zhou, S. (2017a). Synthesis of pyrophoric active ferrous sulfide with oxidation behavior under hypoxic conditions. *Vacuum*, *143*, 386–394. https://doi.org/10.1016/j.vacuum.2017.07.001

Gao, J., Man, X., Shen, J., Meng, Q., & Zhou, S. (2017b). Synthesis of pyrophoric active ferrous sulfide with oxidation behavior under hypoxic conditions. *Vacuum*, *143*, 386–394. https://doi.org/10.1016/j.vacuum.2017.07.001

Gerald William Wellman, Brian Matthew Melof, Anay Josephine Luketa-Hanlin, & Marion Michael Hightower. (2004). *Guidance on risk analysis and safety implications of a large liquefied natural gas (LNG) spill over water*.

GHS. (2017). *Hazard Communication Information Sheet reflecting the US OSHA Implementation of the Globally Harmonized System of Classification and Labelling of Chemicals (GHS)*. https://www.osha.gov/dsg/hazcom/index.html

Globally Harmonized System (GHS) of Classification and Labeling of Chemicals Produced by SCHC-OSHA Alliance GHS Information Sheet Workgroup What is the GHS? (2010). http://www.osha.gov/dsg/hazcom/ghs.html

Globally Harmonized System of Classification and Labeling of Chemicals (GHS) . (2009).

Gonçalves, R. F. B., Iha, K., & Rocco, J. A. F. F. (2018a). Reactive molecular dynamics simulation and chemical kinetic evaluation of combustion of triethylaluminium (TEA). *Quimica Nova*, *41*(5), 507–511. https://doi.org/10.21577/0100-4042.20170200

Gonçalves, R. F. B., Iha, K., & Rocco, J. A. F. F. (2018b). Reactive molecular dynamics simulation and chemical kinetic evaluation of combustion of triethylaluminium (TEA). *Quimica Nova*, *41*(5), 507–511. https://doi.org/10.21577/0100-4042.20170200

Gonçalves, R. F. B., Iha, K., & Rocco, J. A. F. F. (2018c). Reactive molecular dynamics simulation and chemical kinetic evaluation of combustion of triethylaluminium (TEA). *Quimica Nova*, *41*(5), 507–511. https://doi.org/10.21577/0100-4042.20170200

HEALTH HAZARD INFORMATION Acute Health Effects. (n.d.). http://www.state.nj.us/health/eoh/odisweb/

Heck & Johnson. (1962). *Aluminium alkyls—safe handling*.

Heyn, A. (2015). Fire protection concept for the storage of pyrophoric materials. In *SYMPOSIUM SERIES*.

Irving Sax, R. J. L. S. 1988. (1988). *Dangerous properties of industrial materials*.

J. Casal, M. G.-M. M. M. A. P. (2012). *"Jet Fires: a 'Minor' Fire Hazard?"*

Karel Van Acker, & Michael Augustinus. (2018). *Impact of bio-based plastics on current recycling of plastics*.

Kong, D., Liu, P., Ping, P., & Chen, G. (2016). Evaluation of the pyrophoric risk of sulfide mineral in storage. *Journal of Loss Prevention in the Process Industries*, *44*, 487–494. https://doi.org/10.1016/j.jlp.2016.08.010

Leong, W. L., & Edwards, R. (2020). *Pyrophorics (Environmental.Health.Safety)*. http://ehs.mit.edu/

Liu, G. R., Lu, W., Wang, N., & Zhou, T. (2013). Study on mechanics analysis of underwater explosion of triethylaluminium. *Applied Mechanics and Materials*, *340*, 401–406. https://doi.org/10.4028/www.scientific.net/AMM.340.401

McGrattan, K. B. (2006). *Fire dynamics simulator (version 4)*. https://doi.org/10.6028/NIST.SP.1018

Mcgrattan, K. B., Baum, H. R., & Hamins, A. (2000). *Thermal radiation from large pool fires*.

McGrattan, K. B., & Forney, G. P. (2004). *Fire dynamics simulator (version 4) :* https://doi.org/10.6028/NIST.SP.1019

McKee, R. H., Adenuga, M. D., & Carrillo, J. C. (2015). Characterization of the toxicological hazards of hydrocarbon solvents. In *Critical Reviews in Toxicology* (Vol. 45, Issue 4, pp. 273–365). Informa Healthcare. https://doi.org/10.3109/10408444.2015.1016216

Mellon, C. (2019). *Pyrophoric handling procedure*. www.cmu.edu/ehs

Mirviss, R. S. & O. (1961). *Safety-pyrophoric organometallics*.

Morgan J.Hurley. (2004). *Hand book of fire protection engineering*.

Muñoz, M., Planas, E., Ferrero, F., & Casal, J. (2007). Predicting the emissive power of hydrocarbon pool fires. *Journal of Hazardous Materials*, *144*(3), 725–729. https://doi.org/10.1016/j.jhazmat.2007.01.121

National Center for Environmental Health (NCEH). (2018). *CDC | Facts about benzene*. https://emergency.cdc.gov/agent/benzene/basics/facts.asp

NFPA. (1994). *N-HEXANE | CAMEO Chemicals | NOAA*. https://cameochemicals.noaa.gov/chemical/851

NIH. (2022). *Octane summary*. https://pubchem.ncbi.nlm.nih.gov/compound/octane

NIST. (2022a). *Benzene*. https://webbook.nist.gov/cgi/cbook.cgi?ID=C71432&Mask=2

NIST. (2022b). *n-Hexane*. https://webbook.nist.gov/cgi/cbook.cgi?ID=C110543&Mask=7

NIST. (2022c). *Octane*. https://webbook.nist.gov/cgi/cbook.cgi?ID=C111659&Mask=2

Nouryon. (2021). *Product Data Sheet of TEA*.

ROTH. (2015). *N-Octane safety data sheet*.

Ryan Schuessler. (2016). *Drones offer hope for fighting Arctic oil spills*.

Sam Mannan Harry H West Mary Kay O, B. M. (n.d.). *Spontaneous Combustible Substances: a Database Update*.

Sam Mannan Harry H West Mary Kay O, B. M. (1999). *Spontaneous Combustible Substances: a Database Update*.

Sato, Y., Okada, K., Akiyoshi, M., Tokudome, K., & Matsunaga, T. (2011a). Reaction hazards of triethylaluminum under closed conditions. *Journal of Loss Prevention in the Process Industries*, *24*(5), 656–661. https://doi.org/10.1016/j.jlp.2011.05.009

Sato, Y., Okada, K., Akiyoshi, M., Tokudome, K., & Matsunaga, T. (2011b). Reaction hazards of triethylaluminum under closed conditions. *Journal of Loss Prevention in the Process Industries*, *24*(5), 656–661. https://doi.org/10.1016/j.jlp.2011.05.009

Soul, F. D. (2021). *TEA Safety Data Sheet*. Thermofisher Scientific.

Stoffen, P. G. (1997). *Methods for the calculation of Physical Effects (Yellow book)*.

Streitwieser & Heathcock. (1989). *Introduction to organic chemistry*.

Technical Bulletin AL-164. (1995). *Handling Pyrophoric Reagents*.

T.W.Rayan, S. T. S. W. W. H. (1992). *Ignition delays, heats of combustion, and reaction rates of Alumium alkyl dervatives used as ignition and combustion enhances for supersonic combustion (NASA-18191)*.

University of Nebraska Lincoln (UNL). (2009). *Safe Operating Procedure*. http://ehs.unl.edu

Urben. (2007). *Reactive chemical hazards*.

10. Anexo A

10.1. TEA input code

```
&HEAD CHID='tea-sample', TITLE='pool fire of TEA' /

------- 1M0.05CS ---------------------------------

MESH IJK=25,25,75, XB=-5,5,-5,5,0.0,30 / 40 cm

&MESH IJK=33,33,99, XB=-5,5,-5,5,0.0,30 / 30 cm

MESH IJK=50,50,150, XB=-5,5,-5,5,0.0,30 / 20 cm

MESH IJK=100,100,300, XB=-5,5,-5,5,0.0,30 / 10 cm

&TIME T_END=100. /

TIME T_END=150. /

&DUMP DT_DEVC=5., DT_HRR=1. /

&MISC SIMULATION_MODE='LES' /

&SPEC ID = 'TEA', FORMULA = 'C6H15Al' /

&SPEC ID = 'ALUMINATE', FORMULA = 'AlO2' /

&SPEC ID = 'OXYGEN', LUMPED_COMPONENT_ONLY = .TRUE. /

&SPEC ID = 'NITROGEN', LUMPED_COMPONENT_ONLY = .TRUE. /

&SPEC ID = 'WATER VAPOR', LUMPED_COMPONENT_ONLY = .TRUE. /

&SPEC ID = 'CARBON MONOXIDE', LUMPED_COMPONENT_ONLY = .TRUE. /

&SPEC ID = 'CARBON DIOXIDE', LUMPED_COMPONENT_ONLY = .TRUE. /

&SPEC ID = 'SOOT',FORMULA='C', LUMPED_COMPONENT_ONLY = .TRUE. /
```

```
&SPEC ID='AIR', BACKGROUND=.TRUE.
    SPEC_ID(1)='OXYGEN', VOLUME_FRACTION(1)=6.25,
    SPEC_ID(2)='NITROGEN', VOLUME_FRACTION(2)=23.51 /

&SPEC ID='PRODUCTS',
    SPEC_ID(1)='ALUMINATE', VOLUME_FRACTION(1)=1.0,
    SPEC_ID(2)='WATER VAPOR', VOLUME_FRACTION(2)=7.5,
    SPEC_ID(3)='CARBON MONOXIDE', VOLUME_FRACTION(3)=1.0,
    SPEC_ID(4)='CARBON DIOXIDE', VOLUME_FRACTION(4)=1.0,
    SPEC_ID(5)='SOOT', VOLUME_FRACTION(5)=4.0,
    SPEC_ID(6)='NITROGEN', VOLUME_FRACTION(6)=23.51 /
&REAC FUEL='TEA', HEAT_OF_COMBUSTION=44694, SPEC_ID_NU='TEA','AIR','PRODUCTS',
NU=-1,-1,1 /
&MATL ID          = 'STEEL'
    EMISSIVITY    = 1.0
    DENSITY       = 7850
    CONDUCTIVITY  = 45.8
    SPECIFIC_HEAT = 0.46 /
&SURF ID       = 'TEA POOL'
    COLOR      = 'YELLOW'
     SPEC_ID(1)='TEA',
     MASS_FLUX(1)=0.053,/
```

```
&SURF ID       = 'STEEL SHEET'
    COLOR    = 'BLACK'
    MATL_ID  = 'STEEL'
    BACKING  = 'EXPOSED'
    THICKNESS = 0.003 /
&VENT MB='XMIN', SURF_ID = 'OPEN' /
&VENT MB='XMAX', SURF_ID = 'OPEN' /
&VENT MB='YMIN', SURF_ID = 'OPEN' /
&VENT MB='YMAX', SURF_ID = 'OPEN' /
&VENT MB='ZMAX', SURF_ID = 'OPEN' /
&OBST XB=-2,2,-2.5,2.5,0.00,0.30, SURF_IDS='TEA POOL','STEEL SHEET','STEEL SHEET' / SURF_IDS ='TOP', 'SIDES', BOTTOM'
&OBST XB=-2,-2,-2.50,2.50,0.00,0.30, SURF_ID='STEEL SHEET' /
&OBST XB=2,2,-2.50,2.50,0.00,0.30, SURF_ID='STEEL SHEET' /
&OBST XB=-2,2,-2.50,-2.50,0.00,0.30, SURF_ID='STEEL SHEET' /
&OBST XB=-2,2,2.50,2.50,0.00,0.30, SURF_ID='STEEL SHEET' /
&SLCF PBY=0.0, QUANTITY='TEMPERATURE', VECTOR=.TRUE. /
&SLCF PBY=0.0, QUANTITY='HRRPUV' /
&BNDF QUANTITY='WALL TEMPERATURE' /
&DEVC XB=0.0,0.0,0.0,0.0,0.3,30, QUANTITY='TEMPERATURE', POINTS=38, Z_ID='Height', ID='TEMPERATURE'/
&DEVC XB=0.0,0.0,0.0,0.0,0.3,30, QUANTITY='GAUGE HEAT FLUX GAS', POINTS=38, Z_ID='Height', ID='HEAT FLUX'/
```

&DEVC XB=-2.50,2.50,-2.50,2.50,0.05,0.50, QUANTITY='WALL TEMPERATURE', STATISTICS='MEAN', SURF_ID='TEA POOL', ID='Tsurf' /

&DEVC XB=0.0,0.0,0.0,0.0,0.3,30, QUANTITY='HRRPUL', POINTS=38, Z_ID='Height', ID='HRRPUL' /

&TAIL /

10.2. 11%TEA/Isopentane input code

&HEAD CHID='tea-solution-sample', TITLE='pool fire of TEA solution' /

------- 1M0.05CS ----------

MESH IJK=25,25,75, XB=-5,5,-5,5,0.0,30 / 40 cm

&MESH IJK=33,33,99, XB=-5,5,-5,5,0.0,30 / 30 cm

MESH IJK=50,50,150, XB=-5,5,-5,5,0.0,30 / 20 cm

MESH IJK=100,100,300, XB=-5,5,-5,5,0.0,30 / 10 cm

&TIME T_END=100. /

&DUMP DT_DEVC=5., DT_HRR=1. /

&MISC SIMULATION_MODE='LES' /

&SPEC ID = 'TEA', FORMULA = 'C6H15Al' /

&SPEC ID = 'ALUMINATE', FORMULA = 'AlO2' /

&SPEC ID = 'OXYGEN', LUMPED_COMPONENT_ONLY = .TRUE. /

&SPEC ID = 'NITROGEN', LUMPED_COMPONENT_ONLY = .TRUE. /

&SPEC ID = 'WATER VAPOR', LUMPED_COMPONENT_ONLY = .TRUE. /

&SPEC ID = 'CARBON MONOXIDE', LUMPED_COMPONENT_ONLY = .TRUE. /

&SPEC ID = 'CARBON DIOXIDE', LUMPED_COMPONENT_ONLY = .TRUE. /

```
&SPEC ID = 'SOOT',FORMULA='C', LUMPED_COMPONENT_ONLY = .TRUE. /

&SPEC ID='AIR', BACKGROUND=.TRUE.

    SPEC_ID(1)='OXYGEN', VOLUME_FRACTION(1)=6.25,

    SPEC_ID(2)='NITROGEN', VOLUME_FRACTION(2)=23.51 /

&SPEC ID='PRODUCTS',

    SPEC_ID(1)='ALUMINATE', VOLUME_FRACTION(1)=1.0,

    SPEC_ID(2)='WATER VAPOR', VOLUME_FRACTION(2)=7.5,

    SPEC_ID(3)='CARBON MONOXIDE', VOLUME_FRACTION(3)=1.0,

    SPEC_ID(4)='CARBON DIOXIDE', VOLUME_FRACTION(4)=1.0,

    SPEC_ID(5)='SOOT', VOLUME_FRACTION(5)=4.0,

    SPEC_ID(6)='NITROGEN', VOLUME_FRACTION(6)=23.51 /

&REAC FUEL='TEA SOLUTION', HEAT_OF_COMBUSTION=48110, SPEC_ID_NU='TEA','AIR','PRODUCTS',

NU=-1,-1,1 /

&MATL ID          = 'STEEL'

    EMISSIVITY    = 1.0

    DENSITY       = 7850

    CONDUCTIVITY  = 45.8

    SPECIFIC_HEAT = 0.46 /

&SURF ID       = 'TEA SOLUTION POOL'

    COLOR     = 'YELLOW'

     SPEC_ID(1)='TEA SOLUTION',

     MASS_FLUX(1)=0.087,/
```

```
&SURF ID      = 'STEEL SHEET'
    COLOR    = 'BLACK'
    MATL_ID  = 'STEEL'
    BACKING  = 'EXPOSED'
    THICKNESS = 0.003 /
&VENT MB='XMIN', SURF_ID = 'OPEN' /
&VENT MB='XMAX', SURF_ID = 'OPEN' /
&VENT MB='YMIN', SURF_ID = 'OPEN' /
&VENT MB='YMAX', SURF_ID = 'OPEN' /
&VENT MB='ZMAX', SURF_ID = 'OPEN' /
&OBST XB=-2,2,-2.5,2.5,0.00,0.30, SURF_IDS='TEA SOLUTION POOL','STEEL SHEET','STEEL SHEET' /
SURF_IDS ='TOP', 'SIDES', BOTTOM'
&OBST XB=-2,-2,-2.50,2.50,0.00,0.30, SURF_ID='STEEL SHEET' /
&OBST XB=2,2,-2.50,2.50,0.00,0.30, SURF_ID='STEEL SHEET' /
&OBST XB=-2,2,-2.50,-2.50,0.00,0.30, SURF_ID='STEEL SHEET' /
&OBST XB=-2,2,2.50,2.50,0.00,0.30, SURF_ID='STEEL SHEET' /
&SLCF PBY=0.0, QUANTITY='TEMPERATURE', VECTOR=.TRUE. /
&SLCF PBY=0.0, QUANTITY='HRRPUV' /
&BNDF QUANTITY='WALL TEMPERATURE' /
&DEVC XB=0.0,0.0,0.0,0.0,0.3,30, QUANTITY='TEMPERATURE', POINTS=38, Z_ID='Height',
ID='TEMPERATURE'/
&DEVC XB=0.0,0.0,0.0,0.0,0.3,30, QUANTITY='GAUGE HEAT FLUX GAS', POINTS=38, Z_ID='Height',
ID='HEAT FLUX'/
```

```
&DEVC XB=-2.50,2.50,-2.50,2.50,0.05,0.50, QUANTITY='WALL TEMPERATURE', STATISTICS='MEAN', SURF_ID='TEA SOLUTION POOL', ID='Tsurf' /

&DEVC XB=0.0,0.0,0.0,0.0,0.3,30, QUANTITY='HRRPUL', POINTS=38, Z_ID='Height', ID='HRRPUL' /

&TAIL /
```

10.3. N-Hexane input code

```
&HEAD CHID='n-hexane-sample', TITLE='pool fire of burning N-Hexane' /

------- 1M0.05CS ----------------------------------

MESH IJK=25,25,75, XB=-5,5,-5,5,0.0,30 / 40 cm

&MESH IJK=33,33,99, XB=-5,5,-5,5,0.0,30 / 30 cm

MESH IJK=50,50,150, XB=-5,5,-5,5,0.0,30 / 20 cm

MESH IJK=100,100,300, XB=-5,5,-5,5,0.0,30 / 10 cm

TIME T_END=0. /

&TIME T_END=100 /

&DUMP DT_DEVC=5., DT_HRR=1. /

&MISC SIMULATION_MODE='LES' /

&REAC FUEL             = 'N-HEXANE'
    FYI              = 'N-HEXANE C_6 H_12'
    CO_YIELD         =0.01
    SOOT_YIELD       =0.1
    HEAT_OF_COMBUSTION = 37600 /
&MATL ID           = 'STEEL'
```

```
    EMISSIVITY    = 1.0
    DENSITY       = 7850.
    CONDUCTIVITY  = 45.8
    SPECIFIC_HEAT = 0.46 /
&SURF ID       = 'N-HEXANE POOL'
    COLOR     = 'YELLOW'
      SPEC_ID(1)='N-HEXANE',
          MASS_FLUX(1)=0.0838, /
&SURF ID       = 'STEEL SHEET'
    COLOR     = 'BLACK'
    MATL_ID   = 'STEEL'
    BACKING   = 'EXPOSED'
    THICKNESS = 0.003 /
&VENT MB='XMIN', SURF_ID = 'OPEN' /
&VENT MB='XMAX', SURF_ID = 'OPEN' /
&VENT MB='YMIN', SURF_ID = 'OPEN' /
&VENT MB='YMAX', SURF_ID = 'OPEN' /
&VENT MB='ZMAX', SURF_ID = 'OPEN' /
&OBST XB=-2,2,-2.5,2.5,0.00,0.30, SURF_IDS='N-HEXANE POOL','STEEL SHEET','STEEL SHEET' /
SURF_IDS ='TOP', 'SIDES', BOTTOM'
&OBST XB=-2,-2,-2.50,2.50,0.00,0.30, SURF_ID='STEEL SHEET' /
&OBST XB=2,2,-2.50,2.50,0.00,0.30, SURF_ID='STEEL SHEET' /
```

&OBST XB=-2,2,-2.50,-2.50,0.00,0.30, SURF_ID='STEEL SHEET' /

&OBST XB=-2,2,2.50,2.50,0.00,0.30, SURF_ID='STEEL SHEET' /

&SLCF PBY=0.0, QUANTITY='TEMPERATURE', VECTOR=.TRUE. /

&SLCF PBY=0.0, QUANTITY='HRRPUV' /

&BNDF QUANTITY='WALL TEMPERATURE' /

&DEVC XB=0.0,0.0,0.0,0.0,0.3,30, QUANTITY='TEMPERATURE', POINTS=38, Z_ID='Height', ID='TEMPERATURE'/

&DEVC XB=0.0,0.0,0.0,0.0,0.3,30, QUANTITY='GAUGE HEAT FLUX GAS', POINTS=38, Z_ID='Height', ID='HEAT FLUX'/

&DEVC XB=-2.50,2.50,-2.50,2.50,0.05,0.50, QUANTITY='WALL TEMPERATURE', STATISTICS='MEAN', SURF_ID='N-HEXANE POOL', ID='Tsurf' /

&DEVC XB=0.0,0.0,0.0,0.0,0.3,30, QUANTITY='HRRPUL', POINTS=38, Z_ID='Height', ID='HRRPUL' /

&TAIL /

10.4. N-Octane input code

&HEAD CHID='n-octane-sample', TITLE='pool fire of burning N-Octane' /

------- 1M0.05CS ----------

MESH IJK=25,25,75, XB=-5,5,-5,5,0.0,30 / 40 cm

&MESH IJK=33,33,99, XB=-5,5,-5,5,0.0,30 / 30 cm

MESH IJK=50,50,150, XB=-5,5,-5,5,0.0,30 / 20 cm

MESH IJK=100,100,300, XB=-5,5,-5,5,0.0,30 / 10 cm

TIME T_END=150. /

&TIME T_END=100 /

&DUMP DT_DEVC=5., DT_HRR=1. /

```
&MISC SIMULATION_MODE='LES' /
&REAC FUEL            = 'N-OCTANE'
    FYI               = 'N-OCTANE C_8 H_18'
    SOOT_YIELD        = 0.04
    HEAT_OF_COMBUSTION = 44420.03 /
&MATL ID          = 'STEEL'
    EMISSIVITY    = 1.0
    DENSITY       = 7850.
    CONDUCTIVITY  = 45.8
    SPECIFIC_HEAT = 0.46 /
&SURF ID       = 'N-OCTANE POOL'
    COLOR      = 'YELLOW'
      SPEC_ID(1)='N-OCTANE',
          MASS_FLUX(1)=0.083, /
&SURF ID       = 'STEEL SHEET'
    COLOR      = 'BLACK'
    MATL_ID    = 'STEEL'
    BACKING    = 'EXPOSED'
    THICKNESS = 0.003 /
&VENT MB='XMIN', SURF_ID = 'OPEN' /
&VENT MB='XMAX', SURF_ID = 'OPEN' /
&VENT MB='YMIN', SURF_ID = 'OPEN' /
```

&VENT MB='YMAX', SURF_ID = 'OPEN' /

&VENT MB='ZMAX', SURF_ID = 'OPEN' /

&OBST XB=-2,2,-2.5,2.5,0.00,0.30, SURF_IDS='N-OCTANE POOL','STEEL SHEET','STEEL SHEET' / SURF_IDS ='TOP', 'SIDES', BOTTOM'

&OBST XB=-2,-2,-2.50,2.50,0.00,0.30, SURF_ID='STEEL SHEET' /

&OBST XB=2,2,-2.50,2.50,0.00,0.30, SURF_ID='STEEL SHEET' /

&OBST XB=-2,2,-2.50,-2.50,0.00,0.30, SURF_ID='STEEL SHEET' /&OBST XB=-2,2,2.50,2.50,0.00,0.30, SURF_ID='STEEL SHEET' /

&SLCF PBY=0.0, QUANTITY='TEMPERATURE', VECTOR=.TRUE. /

&SLCF PBY=0.0, QUANTITY='HRRPUV' /

&BNDF QUANTITY='BURNING RATE' /

&BNDF QUANTITY='WALL TEMPERATURE' /

&DEVC XB=-2.50,2.50,-2.50,2.50,0.05,0.50, QUANTITY='WALL TEMPERATURE', STATISTICS='MEAN', SURF_ID='N-OCTANE POOL', ID='Tsurf' /

&DEVC XB=0.0,0.0,0.0,0.0,0.3,30, QUANTITY='HRRPUL', POINTS=38, Z_ID='Height', ID='HRRPUL' /

&TAIL /

10.5. Benzene input code

&HEAD CHID='banzene-sample', TITLE='pool fire of burning Benzene' /

------- 1M0.05CS ----------

MESH IJK=25,25,75, XB=-5,5,-5,5,0.0,30 / 40 cm

&MESH IJK=33,33,99, XB=-5,5,-5,5,0.0,30 / 30 cm

MESH IJK=50,50,150, XB=-5,5,-5,5,0.0,30 / 20 cm

MESH IJK=100,100,300, XB=-5,5,-5,5,0.0,30 / 10 cm

```
TIME T_END=150. /

&TIME T_END=100 /

&DUMP DT_DEVC=5., DT_HRR=1. /

&MISC SIMULATION_MODE='LES' /

&REAC FUEL             = 'BENZENE'
    FYI              = 'BENZENE C_6 H_6'
    SOOT_YIELD       = 0.03
    HEAT_OF_COMBUSTION = 41831.07 /
&MATL ID          = 'STEEL'
    EMISSIVITY    = 1.0
    DENSITY       = 7850.
    CONDUCTIVITY  = 45.8
    SPECIFIC_HEAT = 0.46 /
&SURF ID       = 'BENZENE POOL'
    COLOR     = 'YELLOW'
      SPEC_ID(1)='BENZENE',
           MASS_FLUX(1)=0.086, /
&SURF ID       = 'STEEL SHEET'
    COLOR     = 'BLACK'
    MATL_ID   = 'STEEL'
    BACKING   = 'EXPOSED'
    THICKNESS = 0.003 /
```

```
&VENT MB='XMIN', SURF_ID = 'OPEN' /

&VENT MB='XMAX', SURF_ID = 'OPEN' /

&VENT MB='YMIN', SURF_ID = 'OPEN' /

&VENT MB='YMAX', SURF_ID = 'OPEN' /

&VENT MB='ZMAX', SURF_ID = 'OPEN' /

&OBST XB=-2,2,-2.5,2.5,0.00,0.30, SURF_IDS='BENZENE POOL','STEEL SHEET','STEEL SHEET' / SURF_IDS
='TOP', 'SIDES', BOTTOM'

&OBST XB=-2,-2,-2.50,2.50,0.00,0.30, SURF_ID='STEEL SHEET' /

&OBST XB=2,2,-2.50,2.50,0.00,0.30, SURF_ID='STEEL SHEET' /

&OBST XB=-2,2,-2.50,-2.50,0.00,0.30, SURF_ID='STEEL SHEET' /

&OBST XB=-2,2,2.50,2.50,0.00,0.30, SURF_ID='STEEL SHEET' /

&SLCF PBY=0.0, QUANTITY='TEMPERATURE', VECTOR=.TRUE. /

&SLCF PBY=0.0, QUANTITY='HRRPUV' /

&BNDF QUANTITY='BURNING RATE' /

&BNDF QUANTITY='WALL TEMPERATURE' /

&DEVC XB=-2.50,2.50,-2.50,2.50,0.05,0.30, QUANTITY='WALL TEMPERATURE', STATISTICS='MEAN',
SURF_ID='BENZENE POOL', ID='Tsurf' /

&DEVC XB=0.0,0.0,0.0,0.0,0.3,30, QUANTITY='HRRPUL', POINTS=38, Z_ID='Height', ID='HRRPUL' /

&TAIL /
```